Prepublished copy

Nature Environment & Pollution Technology

This is a peer-reviewed prepublished version of the paper to be published in Vol. 25, No. 4, December 2026 issue

Original Research Paper

Synthesis and Characterization of Amino Acid-Based Ionic Liquids for Selective Absorption of CO_2 Using Liquid Foam Bed and Semi-Batch Reactors

Santhi Raju Pilli†

Department of Chemical Engineering Technology, College of Applied Industrial Technology, Jazan University, Jazan 45142, Kingdom of Saudi Arabia.

† Corresponding Author: Santhi Raju Pilli; spilli@jazanu.edu.sa; ssanthirajup@gmail.com

https://orcid.org/: 0000-0001-8841-6753

Key Words	CO_2 absorption, Amino acids, Ionic liquids, Foam bed reactor, NMR and Raman Spectra
DOI	https://doi.org/10.46488/NEPT.2026.v25i03.D1912 (DOI will be active only after the final publication of the paper)
Citation for the Paper	Pilli, S.R., 2026. Synthesis and characterization of amino acid-based ionic liquids for selective absorption of CO_2 using liquid foam bed and semi-batch reactors. *Nature Environment and Pollution Technology*, 25(4), D1912. https://doi.org/10.46488/NEPT.2026.v25i03.D1912

Abstract: Carbon dioxide (CO_2) gas emissions were produced by burning fossil fuels for power generation, automobiles, and other major industrial processes. Hence, there is a need for efficient CO_2 absorption using advanced materials and reactor systems within the framework of carbon absorption and storage technologies. This work emphasizes the synthesis and characterization of amino acid-based ionic liquids (AAILs) for CO_2 (99.99% pure) absorption via a liquid foam bed reactor (FBR) and semi-batch equilibrium studies (SBES). Seven different AAILs namely [TETA][ALA], [TETA][LYS], [TETA][GLU], [TETA][GLN], [TETA][MET], and [TETA][PHE] were newly synthesized. The AAILs were characterized using FTIR and Raman spectroscopy, ^{1}H, and ^{13}C NMR spectroscopy to confirm the AAILs. The physical properties, such as viscosity, density, and surface tension of AAILs, were also presented. The highest and lowest densities of 1.170 and 1.0646 g cm^{-3} were observed for [TETA][ASP] and [TETA][ALA], respectively, among synthesized AAILs. The application of AAILs in FBR and SBES for the absorption of CO_2 was performed under different experimental conditions. Parameters such as the effect of initial concentration, the effect of surfactant, and pH, as well as regeneration of AAILs, were studied. [TETA][LYS] gave the highest moles of CO_2 absorbed per mole of [TETA][LYS] used; it is reported that the highest mole ratio of 0.442, 0.172, and 0.112 (dry basis) was observed in the initial concentration of 500, 300 and 100 mmol CO_2, respectively. Finally, it was noted that the highest mole ratio of CO_2 per mole of [TETA][GLU] was obtained at 0.166, followed by 0.133 for [TETA][ALA] during desorption studies.

Graphical abstract

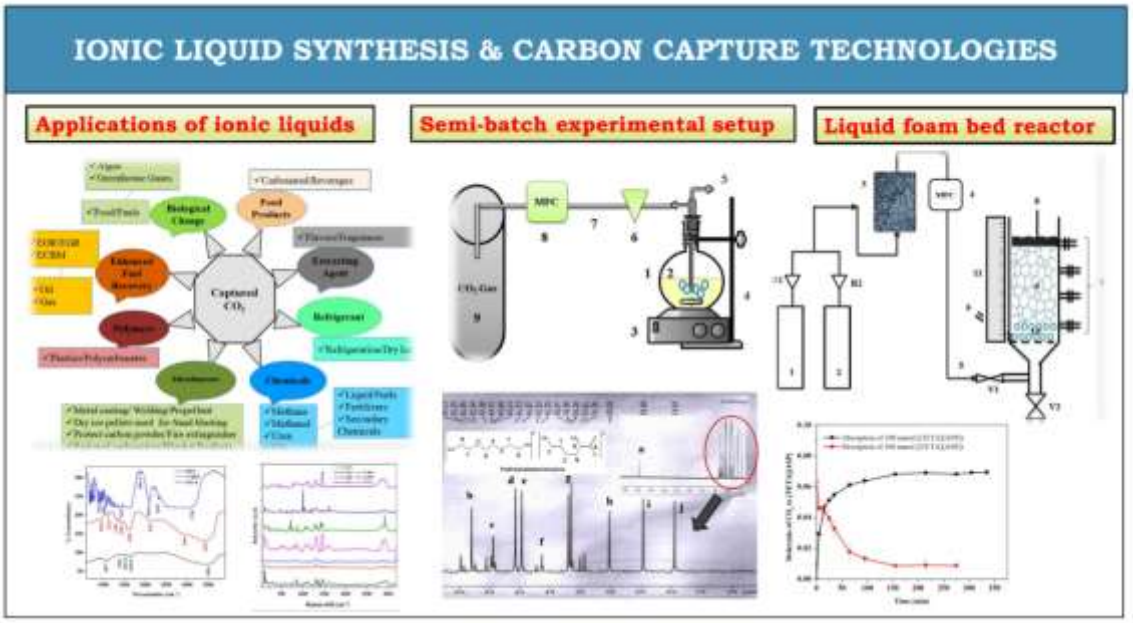

1. INTRODUCTION

The increasing concentration of greenhouse gases (GHGs), particularly carbon dioxide (CO_2), has become a critical global concern due to its significant contribution to climate change. Industrial activities and fossil fuel–based power generation are among the primary sources of CO_2 emissions. In this context, carbon absorption and storage (CCS) has emerged as a vital technological strategy to mitigate CO_2 emissions and limit their release into the atmosphere (Rackley 2010). CCS involves three main stages: (i) absorption of CO_2 from large point sources, (ii) transportation via pipelines or marine systems, and (iii) long-term storage in deep geological formations such as depleted oil and gas reservoirs or saline aquifers (IPCC 2005). This integrated approach enables substantial reductions in emissions while allowing continued use of existing energy infrastructure.

Despite its potential, conventional CO_2 absorption technologies face several limitations. Common absorption approaches–including pre-combustion, post-combustion, and oxy-fuel combustion–are often associated with high energy requirements, operational complexity, and high economic costs. In particular, solvent-based absorption systems using aqueous amines suffer from drawbacks such as solvent degradation, equipment corrosion, and high regeneration energy demand. Additionally, scaling these technologies to match large emission sources remains a major challenge, especially when considering the availability and suitability of storage sites. These limitations highlight the need for more efficient, cost-effective, and sustainable alternatives for CO_2 absorption. Figure 1 illustrates the different products or compounds that can be obtained from absorption CO_2 technologies.

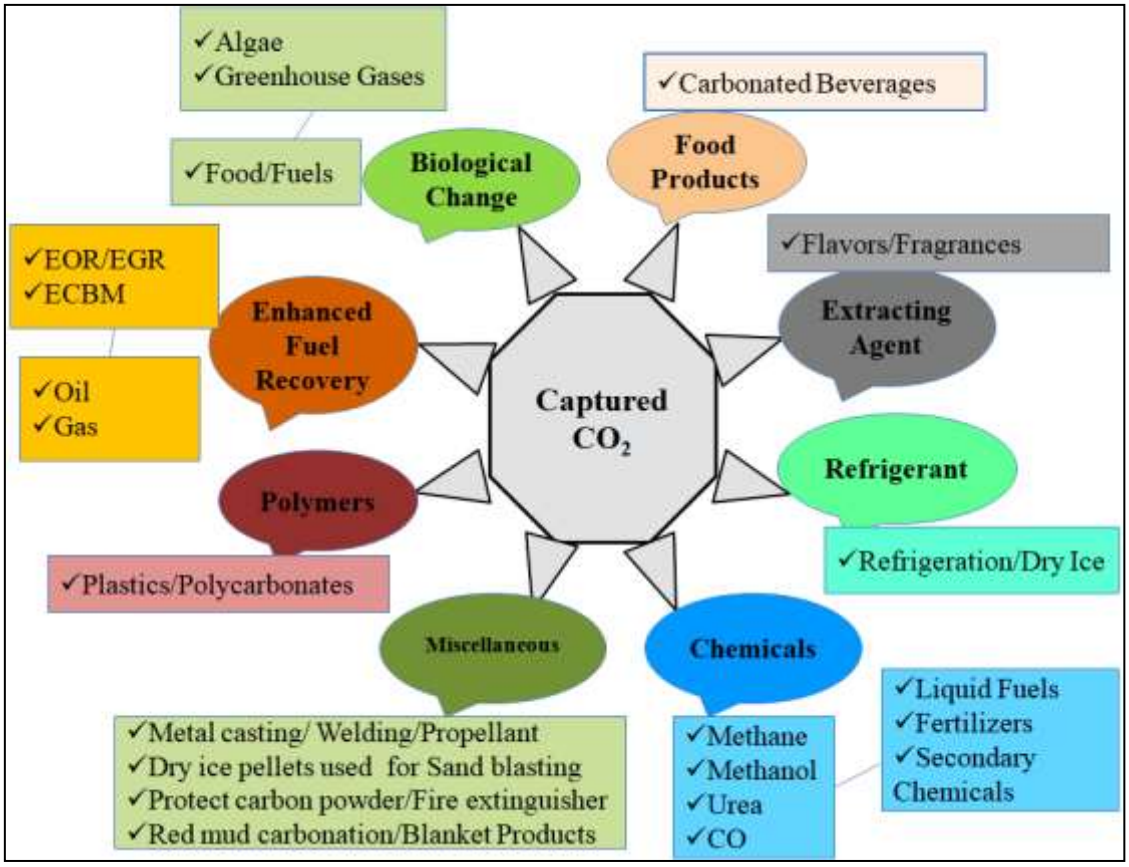

Figure 1. Illustration of various products that can be obtained from CO_2-absorption technologies.

In recent years, ionic liquids (ILs) have gained considerable attention as promising materials for CO_2 absorption due to their unique physicochemical properties, including negligible vapour pressure, high thermal stability, and tunable chemical structures. Among them, amino acid-based ionic liquids (AAILs) have emerged as particularly attractive candidates because they combine the advantages of ILs with enhanced CO_2 affinity and environmental compatibility. AAILs exhibit strong chemical interactions with CO_2, leading to higher absorption capacities and selectivity compared to conventional solvents. Furthermore, their design flexibility allows for optimization of performance characteristics such as viscosity, absorption kinetics, and regeneration efficiency. While ionic liquids have also been explored in areas such as wastewater treatment and membrane separation, these applications are beyond the primary scope of this study and are therefore only briefly acknowledged.

To fully exploit the potential of advanced solvents such as AAILs, there is a growing need for innovative reactor systems that can enhance mass transfer and overall process efficiency. One such promising technology is the foam-bed reactor (FBR), which offers improved gas–liquid contact, higher interfacial area, and enhanced mixing characteristics compared to conventional packed or stirred reactors. The FBR system can significantly improve CO_2 absorption rates while potentially reducing solvent usage and energy consumption. Therefore, integrating AAILs with advanced reactor designs like FBR represents a forward-looking approach to overcoming the limitations of traditional CO_2 absorption systems.

In summary, the development of efficient CO_2 absorption technologies requires a synergistic combination of advanced materials and innovative process design. This study focuses on the application of amino acid-based ionic liquids in a foam-bed reactor system, aiming to provide an effective and sustainable solution for CO_2 absorption.

BACKGROUND RESEARCH

Several carbon absorption technologies have already been accomplished on a lab scale. Some of these are demonstrated industrially and involve different processes involving physisorption or chemisorption (Zhang et al. 2011, Cahyonugroho et al. 2025, Mandal & Bandyopadhyay 2011), ionic liquid membranes and membrane separations (Makino & Kanakubo, 2006; Ramdin et al. 2012, Jones 2011), and molecular sieves (Sarker et al. 2017, Wahby 2012, Mohamedali 2018). The combination of ionic liquid (ILs) and composite materials were utilized for CO_2 absorption (Pilli et al. 2014, Mulk 2023), and amines and amino acid ILs (Du 2016, Qu 2022, Yamini & Khanna 2014, Mumford 2017). The use of novel materials, such as ionic liquids as electrolytes and nanostructured materials for cathodes, has the potential to enhance both the energy efficiency and lifespan of batteries (Padmanabhan et al. 2024).

Most of the literature is available on amine-based technologies. The most used amines for CO_2 absorption are monoethanolamine, diethanolamine, and methyl-diethanolamine, via carbamate/carbonate formation. Even though this kind of conventional CO_2 absorption technology has been operational in the industry for quite some period, some of the exposed defects have yet to be addressed. Nevertheless, repeated drawbacks of these systems include the degradation of expensive solvents, thermal stability, corrosive problems, and consumption of high-power consumption in the regeneration process due to the loss of the solvent by evaporation.

Reviews on IL for CO_2 absorption were reported in the literature (Cota & Martinez 2017). CO_2 adsorption, synthesis, and use of metal-organic frameworks (MOFs) impregnated with ILs were reported in the literature (Lupa et al. 2024). Ionic liquids were also used as a membrane solvent or supported ionic liquid membranes (SILMs) for CO_2 absorption (Makino & Kanakubo, 2006, Ramdin et al. 2012, Sarker et al. 2017, Elmobarak et al. 2023).

1.1. ILs in wastewater treatment and membrane filtration

A variety of polar and non-polar materials, such as organic contaminants, heavy metals, and dyes, which are frequently found in industrial wastewater, can be dissolved by ILs (Zhang et al. 2011, Mandal & Bandyopadhyay 2011). This enables them to remove pollutants from wastewater in an efficient way. ILs have unique properties such as solubility, selectivity, and reusability, making them extremely promising solvents for the treatment of wastewater, effective adsorbents for water treatment, and extraction of contaminants, and membrane filtration, for absorbing and capturing CO_2 (Makino & Kanakubo, 2006, Ramdin et al. 2012, Jones 2011,

Sarker 2017). To reduce expenditures, ensure environmental safety, and solve issues with stability and scalability, their use must be appropriately customized.

Liquid-liquid extraction (LLE), in which pollutants are extracted from water and concentrated in the IL phase, is an example of ILs (Mulk 2023). The IL can then be recycled and used again. For the removal of organic contaminants such as petroleum hydrocarbons or chlorinated chemicals, this method can be highly effective. Targeting various pollutants (such as pesticides, dyes, and medicines) is made possible by the ability to fine-tune the IL's selectivity for specific contaminants through changes to the cation or anion (Sarker 2017, Lupa et al. 2024). Membrane materials can have ionic liquids added to enhance their filtration performance. These modified membranes are more efficient than conventional membranes at removing both organic and inorganic contaminants from wastewater, which increases the effectiveness of methods like nanofiltration and reverse osmosis.

Although the primary focus of this study is CO_2 absorption, the discussion on wastewater treatment highlights the broader environmental applicability of ionic liquids. Their tunable physicochemical properties, low volatility, and potential for recyclability make them promising green solvents not only for pollutant removal but also for gas absorption processes. These characteristics support their selection as effective absorbents in CO_2 absorption systems.

1.2. Biodegradability, Toxicity, reusability, and recovery of ILs

Several ILs can be designed to be biodegradable and non-toxic, which are the key factors for wastewater treatment (Babamohammadi et al. 2015). Conventional organic solvents or chemicals used for wastewater treatment pose long-term environmental effects. However, ILs can be engineered to minimize these risks. Nonetheless, an IL's biodegradability depends on its chemical structure, and some ILs may still be toxic to aquatic organisms (Babamohammadi et al. 2015). Another significant advantage of IL is recyclability. ILs can usually be regenerated using simple methods like evaporation and distillation, after being used to treat wastewater, which minimizes waste and lowers operating costs. Their reusability makes them a sustainable choice in large-scale applications.

In this work, about seven different ionic liquids (ILs) were newly synthesized using amino acids (AAs) as anions and triethylenetetramine (TETA) as a cation. The paragraphs below will describe the details of ILs, amino acids, and amines, and physical properties and applications in science and engineering.

1.3. Amines

Amines (amino alkanes) are, in general, organic substances that have a basic nitrogen atom with a lone pair, derived from ammonia by the substitution of one or more H^+ atoms by organic compounds like alkyl or

aryl groups. There are about four different types: primary, secondary, tertiary, and cyclic amines with elevated melting and boiling points. The industrial applications of amines are widely used in the preparation of dyes and drugs. It was reported that the different amine-based compounds, such as monoethanolamine (MEA), diisopropylamine (DIPA), diglycolamine (DGA), diethanolamine (DEA), and methyl-diethanolamine (MDEA), are widely used in process industries for the removal of CO_2 and hydrogen sulfide (H_2S) from natural gas and petroleum refining process gas streams. Amines were used for the absorption of CO_2 from burning gases and waste gases and have the capability for the removal of greenhouse emissions (Babamohammadi et al. 2015, Fukumoto 2005).

1.4. Amino acids

AAs are simple organic compounds comprising a carboxyl (–COOH) and an amino ($–NH_2$) group. These carboxyl and amino functional groups are also useful in their capacity to introduce functional groups. It is well known that about 20% of the human body contains proteins. These supermolecules play a significant role in all biological processes, and AAs are the building blocks of them. The advantages of AAs are a low environmental impact, high biodegradable nature, negligible volatility, high resistance to oxidative degradation, and lower volatility due to their ionic structure. The physical characteristics of AAs are as follows: crystalline solids with amazingly high melting points (200-300 °C), usually water soluble and insoluble in non-polar organic solvents such as hydrocarbons, possess optical isomers owing to the presence of asymmetric α-carbon atoms, zwitterionic nature (Yamini & Khanna 2015). AA can taste as sweet as bland, or occasionally bitter. AAs are primarily used in cosmetics, active pharmaceutical ingredients (APIs), medical foods or medical nutrition, drinks, culture media, dietary supplements, functional foods, and polymer synthesis. In recent times, these AAs were also used in the synthesis and preparation of ILs (Walden 1914). The list of amino acids used in this study as an ion and amines used as cations is given in Table 1 (a) and (b), respectively.

Table 1(a). List of amino acids that were used as an anion in this study.

S. No.	Compound Name	Synonym/ IUPAC ID	Structure/Formula	CAS No.	Molecular Weight (g mol^{-1})
1.	L-Aspartic acid [ASP]	(S)-(+)-Aminosuccinic acid, (S)-Aminobutanedioic acid	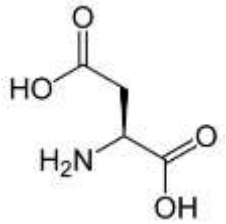 $C_4H_7NO_4$	56-84-8	133.10

2.	L-Alanine [ALA]	(S)-2-Aminopropionic acid	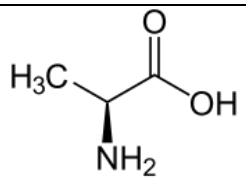 $C_3H_7NO_2$	56-41-7	89.09
3.	Glutamine [GLN]	(S)-2,5-Diamino-5-oxopentanoic acid	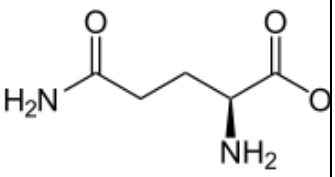 $C_5H_{10}N_2O_3$	56-85-9	146.14
.	Glutamic acid [GLU]	(S)-2-Aminopentanedioic acid	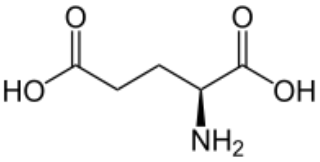 $C_5H_9NO_4$	56-86-0	147.13
5.	L-Lysine [LYS]	(S)-2,6-Diaminohexanoic acid monohydrochloride	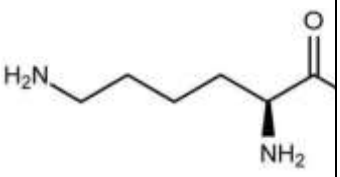 $C_6H_{14}N_2O_2$	657-27-2	182.65
6.	L-Methionine [MET]	(S)-2-Amino-4-(methylmercapto)butyric acid	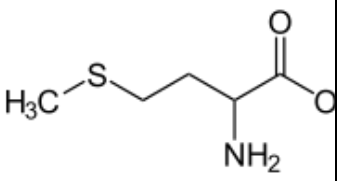 $C_5H_{11}NO_2S$	63-68-3	149.21
7.	L-Phenylalanine [PHE]	(S)-2-Amino-3-phenylpropionic acid	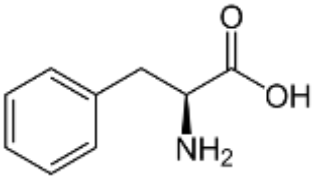 $C_9H_{11}NO_2$	63-91-2	165.19

Table 1(a). List of amines used in this study as cautions.

S. No.	Compound Name	Synonym/ IUPAC ID	Structure/Formula	CAS No.	Molecular Wt. g mol^{-1}	Density g cm^{-3}
1.	Triethylenetetramine [TETA]	N,N'-Bis(2-aminoethyl)-1,2-ethanediamine	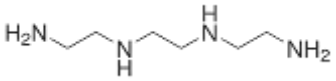 $C_6H_{18}N_4$	112-24-3	146.24	0.982

1.5. Ionic liquids as green solvents

ILs are very attractive and are promptly acquiring research areas in the recent era of science and engineering, especially in modern physical chemistry, as green solvents. These are liquids at ambient temperature, mainly used as a substitute for conventional volatile organic solvents such as tetrachloroethylene, formaldehyde, methylene chloride, benzene, ethylene glycol, toluene, and xylene. Applications for ILs in different fields of science and engineering are presented in Figure 2. ILs are substances prepared with organic cations and both organic and inorganic anions. ILs were reported very first in the year 1914 by Paul Walden, a well-known Latvian chemist, for his work on stereochemical reactions (Walden 1914). ILs have significant attention owing to their notable and eco-friendly properties, small vapour pressures, reusability, broad chemical and thermal stability, non-inflammable nature, high ion density, elevated electrochemical window, tunable viscosity, and superior electrical conductivity (Wilkes 2002). Chemical structures of frequently used cations and anions are presented in Table 1(c). Similarly, Table 2 compares the various characteristics of volatile organic solvents, molten salts, and ILs.

Alternatively, amino acid-based ionic liquids (AAILs) can also be used for better CO_2 absorption capacity. As mentioned above, AAs comprise both a carboxyl (–COOH) and an amino ($–NH_2$) functional group. It was reported that the effect of CO_2 with AAs is alleged to be similar to that of alkanol amines. On the other hand, the precise CO_2 reaction mechanism of AAs is nonetheless a subject of argument in the scientific community. In 2002, Kumar et al. described that the reaction mechanism is different from the zwitterionic mechanism with the hypothesis of a direct 2:1 mechanism producing carbamate and protonated amine as indicated in equation (1) (Kumar et al. 2002).

$$2RNH_2 + CO_2 \underset{k_{2,2}}{\overset{k_{2,1}}{\rightleftharpoons}} RNHCOO^- COO^- + RNH_3^+ \quad (1)$$

However, as described in the literature, a zwitterionic mechanism for CO_2 reacts with potassium salts of glycine and taurine as given in equations 2 and 3 (Kumar et al. 2003).

$$^-OOC\text{-}R\text{-}NH_2 + CO_2 \underset{k_{-1}}{\overset{k_1}{\rightleftharpoons}} {}^-OOC\text{-}R\text{-}N^+H_2COO^- \quad (2)$$

$$^{-}OOC\text{-}R\text{-}N^{+}H_2COO^{-} + B \rightarrow {}^{-}OOC\text{-}R\text{-}NHCOO^{-} + {}^{-}OOC\text{-}R\text{-}NH_3^{+} \quad (3)$$

Where B is any alkali compound. In a non-aqueous medium, AAs behave as a base. In 2010, Gurkan et al. described that the reaction of CO_2 with ILs prepared with amino acids terminates at the disposition of carbamic acid (eq. 4) in the absence of forming carbamate species (eq. 5) (Gürkan et al. 2010). Gurkan et al. have examined the absorption of CO_2 in phosphonium-based cations combined with *methionine* and proline amino acids as anions. They have anticipated that a 1:1 stoichiometric reaction of CO_2 with AAILs, which suggests the reaction ends with the formation of carbonic acid (eq. 4).

$$^{-}OOC\text{-}R\text{-}NH_2 + CO_2 \underset{k_{-1}}{\overset{k_1}{\longleftrightarrow}} {}^{-}OOC\text{-}R\text{-}NHCOOH \quad (4)$$

$$^{-}OOC\text{-}R\text{-}NHCOOH + B \rightarrow {}^{-}OOC\text{-}R\text{-}NHCOO^{-} + {}^{-}OOC\text{-}R\text{-}NH_3^{+} \quad (5)$$

The proposed mechanisms (Eqs. 1-5) are used to interpret experimental trends qualitatively, and detailed mechanistic validation is beyond the scope of the current study.

In other previous work, Yamini and Khanna have studied the CO_2 solubility in different amino acids-based ILs synthesized by butylmethyl imidazolium ($[BMIM]^{+}$) as cation and amino acids as anions (Yamini & Khanna 2015). Goodrich et al. examined the CO_2 absorption of various amino acid-based anions and phosphonium-based cations for preparing the IL and proposed the mechanisms (Goodrich et al. 2022). Kortunov et al. studied physical absorption techniques for CO_2 absorption in ionic liquids, for higher-pressure carbon absorption using imidazolium-based ionic liquids and amine mixing in the ionic liquid solution (Kortunov et al. 2015). As seen above, the majority of the reports were defending the formation of zwitterion intermediate (eq. 2) and (eq. 3) as the main beneficial way instead of one-step carbamate formation (eq. 1) or via carbamic acid formation (eq. 4) and (eq. 5) (Danckwerts 1979, Versteeg & van Swaaij, van Holst et al., 2009, Xie et al., 2010).

The primary goal of this work is to examine the effect of amine-functionalization on different amino acids as an anion. Another reason for selecting the amino acids is that they are biodegradable, easily available, and comparatively low in price, although very few studies have been reported in the literature. In this work, seven different AAILs were synthesized namely: [TETA][ALA], [TETA][ASP], [TETA][LYS], [TETA][GLU], [TETA][GLN], [TETA][MET], and [TETA][PHE]. CO_2 absorption studies were carried out in the FBR at room temperature.

Although amino acid-based ionic liquids (AAILs) have been widely reported, the originality of this work lies in the use of triethylenetetramine (TETA) as a polyamine-based cation combined with various amino acid anions, providing multiple active amine sites that enhance CO_2 interaction. A detailed comparative discussion has been incorporated to evaluate these TETA-based AAILs against commonly reported imidazolium- and phosphonium-based systems in terms of CO_2 absorption capacity, reaction mechanisms (chemisorption versus

physisorption), availability of active sites, and environmental and economic aspects (Yamini & Khanna 2015). Furthermore, the application of these AAILs in a liquid foam-bed reactor (FBR) highlights their functional advantage through improved gas–liquid interfacial contact, reinforcing the distinct contribution of this study.

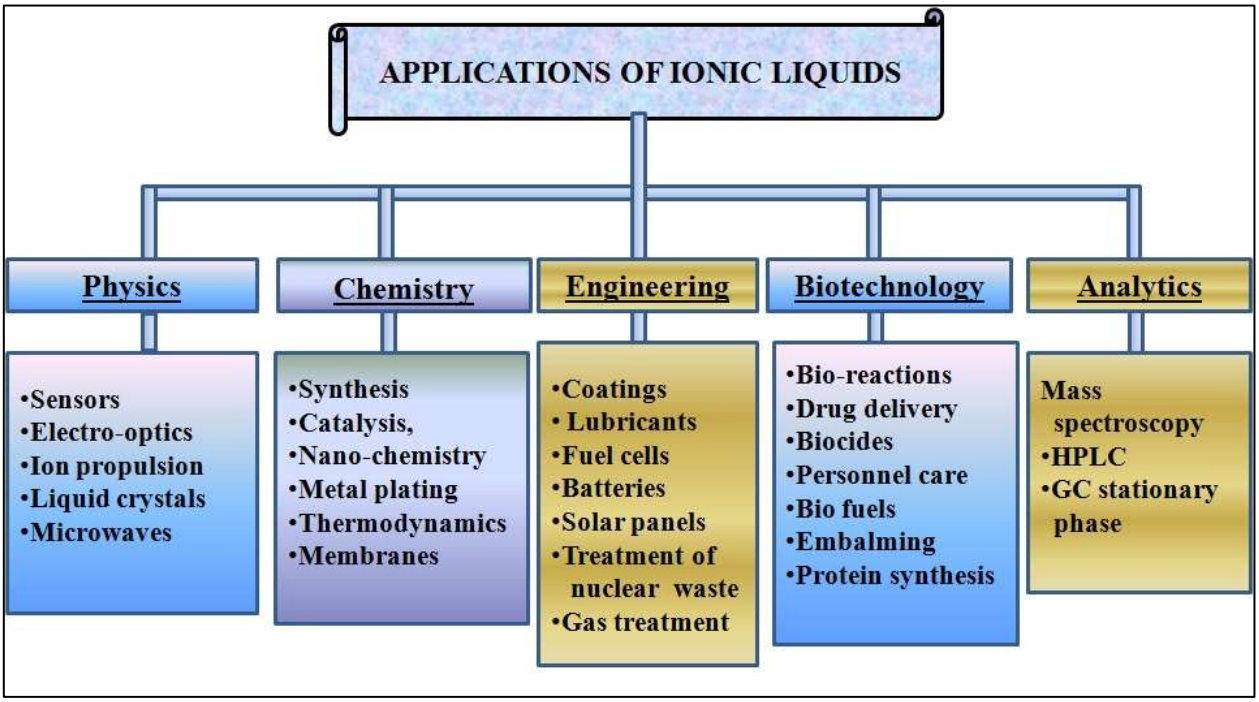

Figure 2. Typical applications of ILs are used in different fields of science and engineering.

Table 1(c). Common anions and cations are utilized in the preparation of ILs.

Anions		
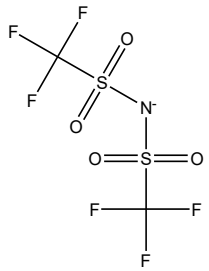 bis(trifluoromethylsulfonyl) amide	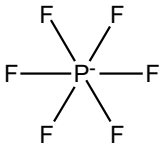 Hexafluorophosphate	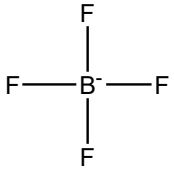 tetrafluoroborate
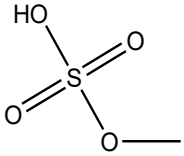 Methylsulfate	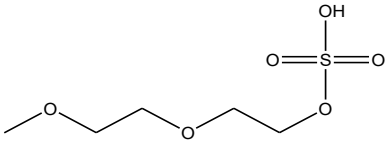 2-2 methoxy ethoxy ethyl sulfate	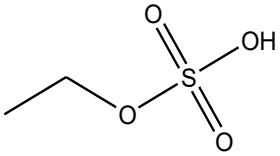 Ethylsulfate

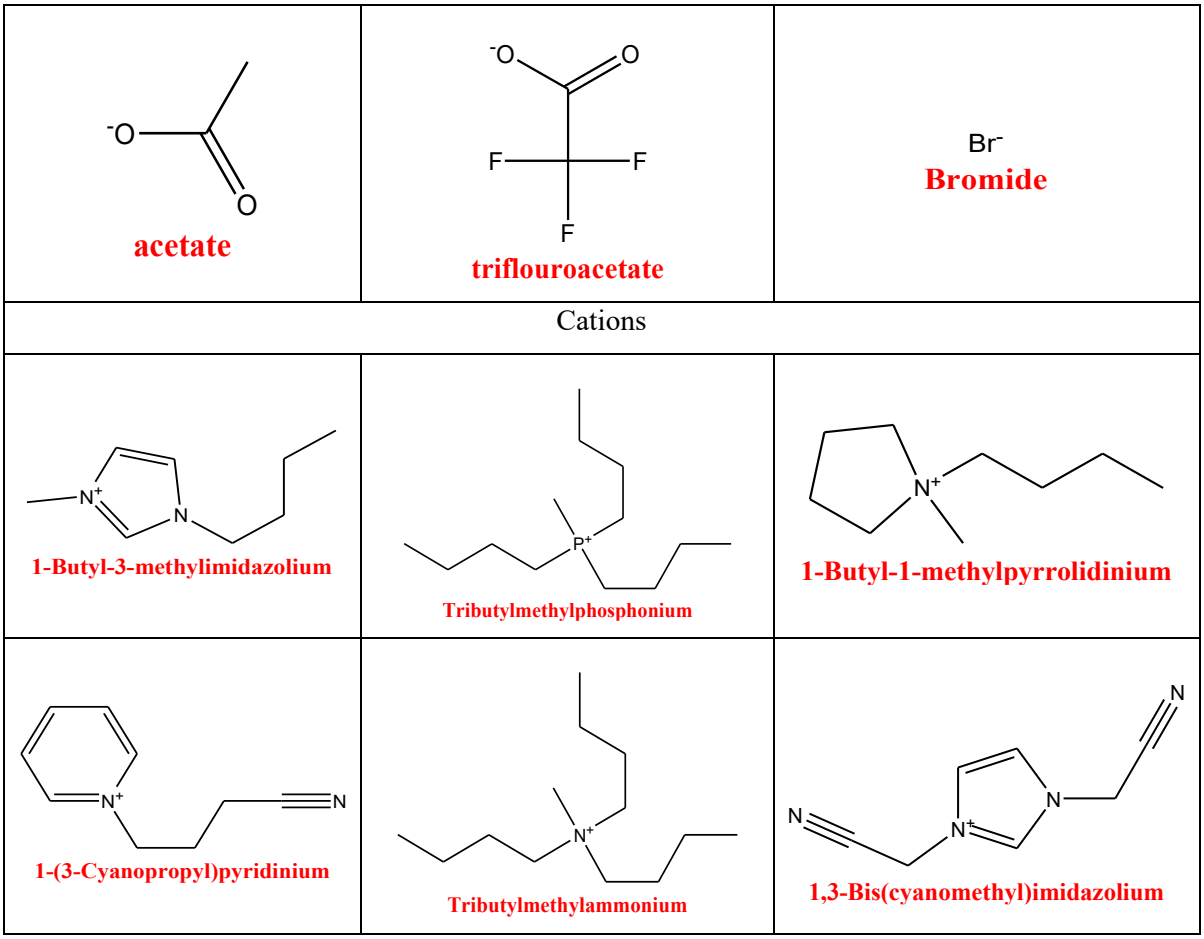

Table 2. Comparison of the various characteristics of volatile organic solvents, molten salts, and ILs.

S. No.	Property	Ionic Liquids	Volatile organic solvents	Molten salts
1	Basic constituents	Pair of ions	Molecules	Pair of ions
2	Application	Multifunction	Single function	Multifunction
3	Catalytic ability	Common and tunable	Rare	Common and tunable
4	Chirality	Common and tunable	Rare	Common and tunable
5	Vapor pressure	Negligible under ambient conditions	Obeys the Clausius-Clepeyron equation	Insignificant under ambient conditions
6	Flammability	Nonflammable	Highly inflammable	Nonflammable
7	Salvation effect	Strong	Week	Strong
8	Cost	Expensive (2-100 times the cost of organic solvents)	Cheap	Expensive
9	Recyclability	Economic imperative	Green imperative	Economic imperative
10	Corrosiveness	Low	Intermediate	High

11	Melting point	-20-150 ℃	<-20℃	> 200 ℃
12	Boling point	< 400 ℃	30-100 ℃	> 400 ℃
13	Viscosity (cP)	Low (22-40, 000)	Low (0.2-100)	High
14	Density ($g\ cm^{-3}$)	High (0.8-3.3)	Medium (0.6-1.7)	High (0.8-3.3)
15	Conductivity	High	Low	High
16	Refractive index	High (1-5-2.2)	Medium (1.3-1.6)	High (1-5-2.2)

2. MATERIALS AND METHODS

All the amino acids, such as L-aspartic acid, L-alanine, L-lysine, L-methionine, L-phenylalanine, glutamine, and glutamic acid, were purchased from CDH, Delhi. Monoethanolamine and triethylenetetramine were also purchased from CDH, Delhi. Dichloro methane, dimethyl ether, sodium lauryl sulfate (SLS), cetrimonium bromide (CTAB), TritonX-100, Tween 80, amyl alcohol, methyl orange indicator, and methanol were procured from Fisher Scientific, India. All the reagents used were as is; no further purification was carried out unless stated.

3. EXPERIMENTAL SECTION

3.1. Synthesis and purification of ionic liquids

AAILs were prepared by H^+ transfer between a Bronsted acid and a Bronsted base. An equimolar quantity of acid and base were reacted with each other. The drop-wise addition of the amine to the amino acid was performed in an ice bath since the reactions are very exothermic; due care was taken while working on the synthesis. At room temperature, the reaction mixture was agitated for a whole day. A small excess of amine was introduced, and it was subsequently removed along with the water by heating it to 80–85 °C to ensure the complete reaction. To remove the unreacted acid and water, the reacted mixture was additionally dried at 80–85 °C under vacuum (about 300 mm Hg), and the residue was subsequently extracted using diethyl ether (DE) or dichloromethane (DCM). Following the evaporation of the solvent, the product was dried for at least three to five days at 80 to 85 °C in a vacuum oven to remove any remaining moisture. Now the AAILs are ready for further characterization and use. The synthesis reactions were conducted without any solvent; if required, 10% methanol was used to dissolve the amino acid in deionized water (if it is in a solid state), stirred for 10-15 h, then added dropwise to TETA. A similar procedure was used for the synthesis of all the AAILs.

3.2. Proposed reaction mechanisms of synthesized ILs

The reaction mechanism between triethylenetetramine and lysine is shown in Scheme 1. TETA consists of a long carbon chain with two primary (–NH_2) groups and two secondary (–NH) groups in it, whereas aspartic acid has two carboxylic groups (–COOH) and one amine group. When aspartic acid is reacted with [TETA], aspartic acid may try to donate protons to [TETA], where the [TETA][ASP] forms. It is proposed that all the amino acids will react with TETA and form AAILs. Other compound reactions such as [TETA][ALA], [TETA][LYS], [TETA][GLU], [TETA][GLN], [TETA][MET], and [TETA][PHE] were given in the supporting information, SI-scheme 1-4.

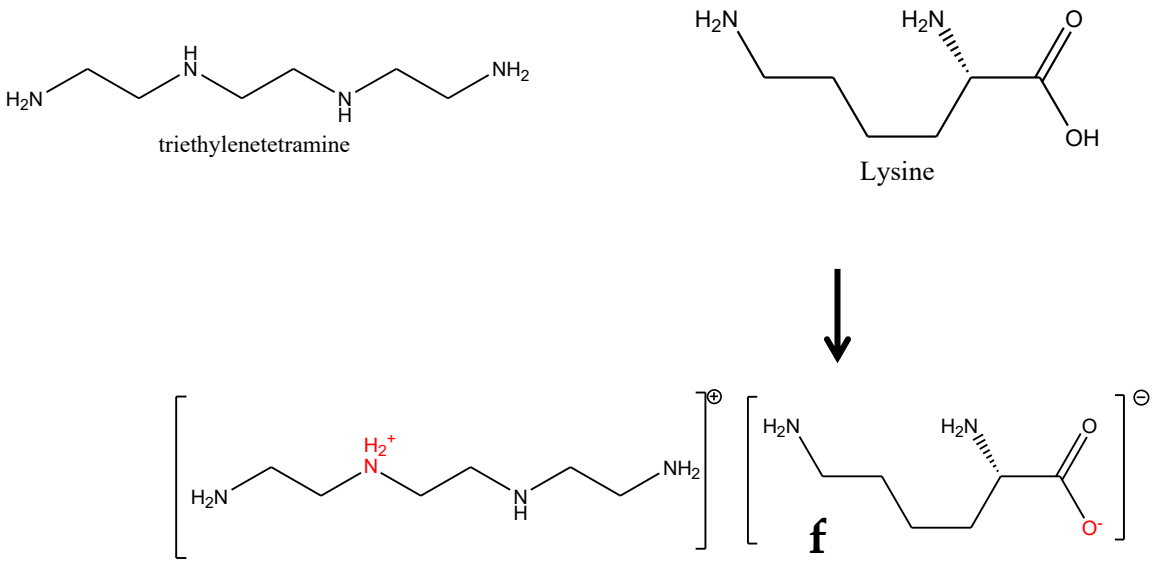

Scheme 1: Proposed reaction mechanisms of [TETA][LYS].

3.3. Procedure for semi-batch equilibrium studies

Equilibrium experiments were conducted in a 250 ml round-bottom flask (RBF) with a lid arrangement by continuous gas supply in and out of the RBF. A known amount of prepared AAIL was taken into the RBF. The desired amount of CO_2 gas was bubbled continuously into the AAIL present in the RBF. Unreacted gas will go out through the vent line of the RBF as shown in Figure 3(a). The entire setup was kept on the magnetic stirrer with the help of the stand. Semi-batch equilibrium experiments for the absorption of CO_2 were carried out for several hours until the equilibrium was reached. Samplings were drawn at predefined time intervals and examined by titrimetry against 2 M HCl in the Chittick apparatus. For each sample, the amount of CO_2 absorbed with time was calculated, and then the moles of CO_2 absorbed for each mole of AAIL. A similar procedure was used to carry out equilibrium experiments for different AAILs.

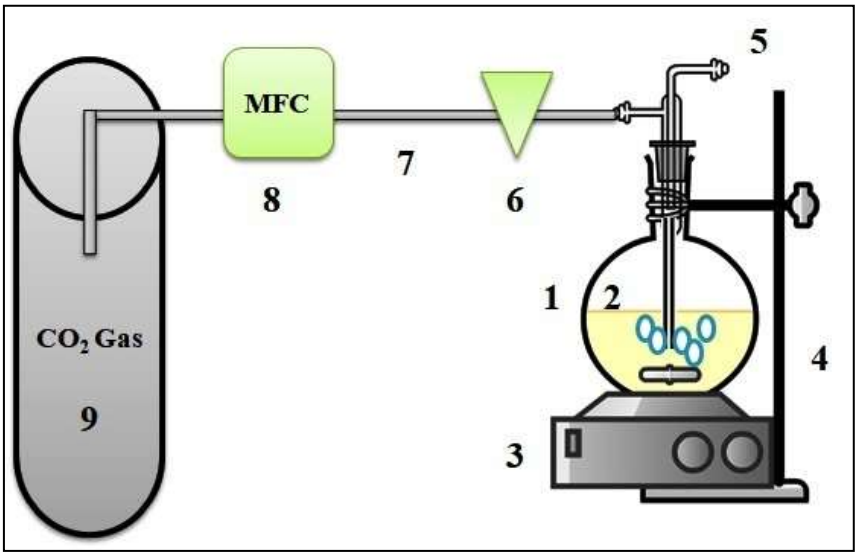

Figure 3(a). Semi-batch equilibrium experiment setup used for CO_2 absorption. (Parts of the figure are as follows: 1. Round bottom flask, 2. Ionic liquid, 3. Magnetic stirrer, 4. Stand, 5. Gas flow out, 6. Rotameter, 7. Gas flow in, 7. Mass flow controller with a digital indication, and 9. CO_2 gas cylinder.

3.4. Regeneration of AAILs

Regeneration of used AAILs was carried out and further used for multiple cycles. Regeneration was done by heating the AAIL at 80 to 90 °C with continuous stirring. During the regeneration, samples were drawn for analysis at fixed time intervals. The rate of desorption was also studied with time. It was observed that AAILs, once regenerated, can be used for a further cycle. The apparatus used for the regeneration of AAILs is presented in Figure 3(b).

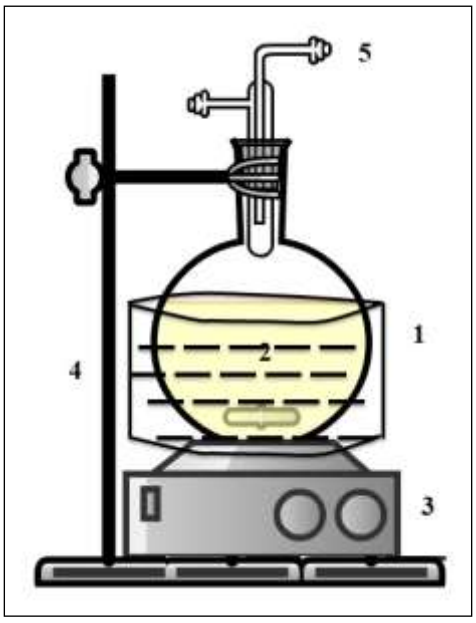

Figure 3(b). The apparatus is used for the regeneration of AAILs. (Parts of the figure are as follows: 1. Round bottom flask, 2. Ionic liquid, 3. Magnetic stirrer, 4. Stand, and 5. Gas flows out to storage.

3.5. Experimental procedure of the liquid foam-bed reactor

CO_2 absorption experiments were carried out in a semi-batch liquid foam-bed reactor (FBR). The experimental model setup of the liquid foam bed reactor used in this study is shown in Figure 4(a). The details of the FBR are as follows. FBR consists of two sections, i.e., the foam section and the storage section. It is a simple, transparent glass column (0.7 m height and 7.6×10^{-2} m diameter) fixed with a distributed plate above the cone-shaped bottom (flow stabilization chamber) as seen in Figure 4. The distributor plate contains several holes in it, which allow the CO_2 gas/air into the column while experimenting. FBR also has one sample charging port above the distributor plate and several sampling ports at different heights for drawing samples for analysis during the experiment.

During the FBR experiments, the regulator of the CO_2 gas cylinder was kept under heating with infrared lamps. This heating will avoid the choking of the gas pipeline due to the formation of dry ice in it. An air compressor was employed to provide the air and dilute the CO_2 gas. Pre-calibrated rotameters were used to measure CO_2 and airflow rates. As mentioned above, CO_2 gas was diluted by mixing air using the packed bed setup, which consists of glass rasching rigs. This packaged bed will be useful for mixing CO_2 and air and preventing dust or solid particles, if any, in the air before it passes through the FBR.

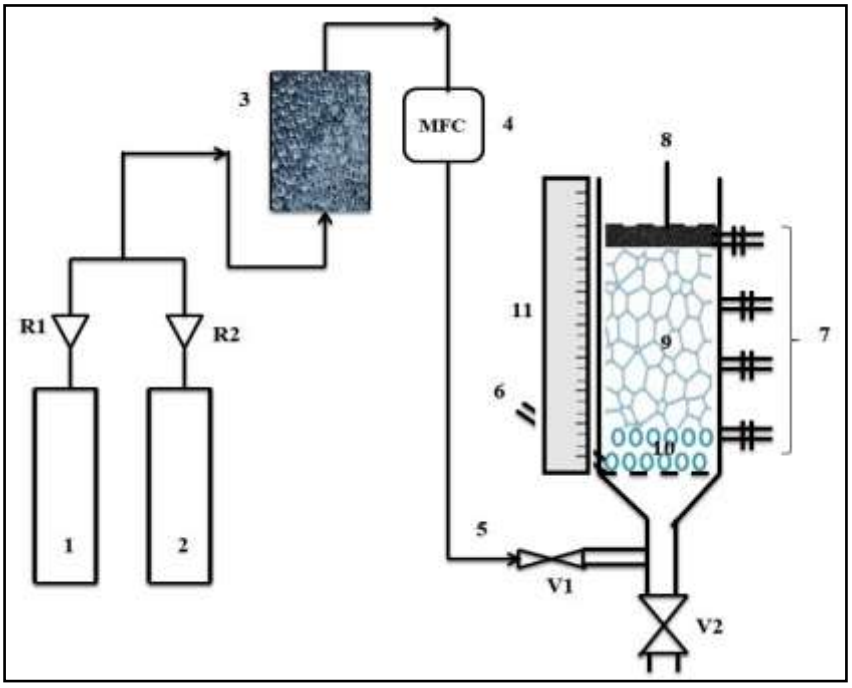

Figure 4(a). Experimental setup of liquid foam bed reactor used in this study. (Parts are as follows: 1. Pure CO_2 gas supply, 2. Air supply, 3. Air and CO_2 mixture (packed bed with glass beads) 4. Mass flow controller with a digital indication, 5. Gas inlet, 6. Liquid charging port, 7. Sampling ports, 8. Sieve plate for from braking, 9. Foam section, 10. Storage section, 11. Ruler, R1 and R2 gas Rotameters, and V_1 and V_2 Valves).

At the very first, the known flow rate of air is released to the FBR. About 100 ml of aqueous AAIL of known concentration was mixed with a known amount of surfactant in a volumetric flask, stirred for 2-3 h and then charged into the FBR through the liquid inlet port. Now the height of the form was monitored. After reaching the desired foam height, CO_2 gas was released from the cylinder and passed through the FBR. CO_2 gas was mixed with air before entering the FBR. Once the CO_2 gas enters the FBR, the experiment starts, and the time is to be noted. At the time of the experiment, the CO_2 gas and air flow rates were monitored with a digital mass flow controller and rotameter, respectively. The height of the foam was maintained by the circularly shaped foam breaker, which consists of 7.5×10^{-2} m diameter sieve plate tagged by the circular sponge (foam, ~7.8×10^{-2} m) on it, connected with about 0.8 m long thin iron rod as shown in the figure. A few drops of amyl alcohol were used in the foam breaker sponge as an anti-foaming agent. When the bubbles of foam reach the foam breaker surface, they will collapse. The sieve plate's perforations will allow the unreacted CO_2 gas to escape. Through the Platea boundaries, the liquid in the foam films will return to the storage section. With the help of a stopwatch, liquid samples were collected at regular time intervals from the sampling ports near storage sections. The CO_2 experiments were continued for 30 min. Then the gas supply was closed, and the solution from the storage section was drained.

CO_2 loading in the given sample of AAIL solution was calculated using the following equation:

$$\alpha = \frac{\left(760\ mmHg - \mathrm{P_{H_2O}}\right)\left(V_{CO_2} - V_{HCl}\right)}{\left(\text{sample vol.(ml)} \times R \times \mathrm{T}\right)} \times 1000$$

Where,

α = CO_2 loading (mole CO_2 per ml of absorbent).

760 mm Hg= 1 atm (standard atmospheric pressure).

P_{H_2O}= Vapour pressure (mm Hg) at temperature 302 (K).

V_{CO_2}= Volume of the displaced solution by CO_2 in the graduated tube (ml).

V_{HCl}= Volume of HCl used for titration (ml).

Sample Vol.= Volume of sample drawn from the FBR (ml).

T=Temperature K.

R=Universal gas constant ($L\cdot torr\ mol^{-1}\cdot K^{-1}$).

3.6. Analysis of Samples

After collecting the samples from FBR experiments at regular time intervals, analysis of CO_2 absorbed was carried out by the Chittick apparatus, as shown in Figure 4(b). For the analysis, a magnetic stirrer, 25 ml conical flask, 50 ml burette, 10 ml pipette, glass stopper, graduated glass tube with indication of scale, glass reservoir, analytical balance (AUW-220D Dual-range semi-micro balance) and methyl orange indicator were used. Then, a collected sample of known weight was taken in a 25 ml conical flask; one or two drops of methyl orange were added and titrated against the 2N HCl by putting the entire setup on a magnetic stirrer, until it turned from yellow to a pale orange colour. The burette reading and gas displaced in the glass reservoir were noted for each

sample, with the time at which the sample was collected. Teflon tape or vacuum grease was used on the conical flask to prevent gas leakage. During the analysis, due care was taken to avoid the leakage of CO_2 gas from the flask.

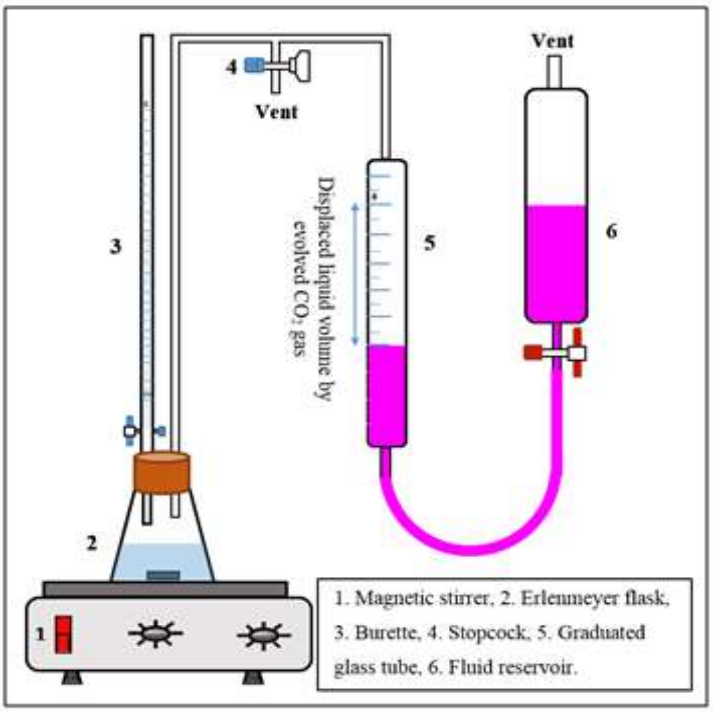

Figure 4(b). Pictorial representation of the Chittick Apparatus used for liquid sample analysis (Norouzbahari et al. 2016).

4. RESULTS OR RESULTS AND DISCUSSIONS

4.1. Characterization of ionic liquids

4.1.1. FTIR analysis

Fourier–transform infrared spectroscopic technique (FTIR) (NICOLET iS50FT-IR model) was carried out to identify the functional groups present in the prepared AAILs by an infrared spectrum of absorption. The FTIR spectra were recorded from wavenumbers 500 to 4000 cm^{-1}. These infrared absorption bands spot the molecular component structures. Figure 5(a) to 5(e) represents the FTIR spectra of the pure [TETA] used as cation, AAs used as anion and synthesized AAILs, namely, [TETA][ALA], [TETA][ASP], [TETA][GLU], [TETA][LYS], [TETA][MET] and [TETA][PHE]. FTIR spectra shows all the major functional groups present in the individual compounds and the prepared AAILs. The distinct FTIR peak representing C=O of –COO present in the amino acid in 1700 and 1462 cm^{-1}, and a peak corresponding to N–H stretching vibration of $–NH_2$ at 3600 to 3000 cm^{-1} range were identified for almost all the AAILs (Barth 200). The FTIR bands of synthesized AAILs were very similar and presented the same spectrum of bands with different wavenumbers. Figure 5(a) shows the FTIR spectra of pure anion $[ALA]^-$, pure cation $[TETA]^{+\cdot}$ and synthesized [TETA][ALA]. The characteristic FTIR

peak corresponding to C=O of –COO at 1647–1400 cm^{-1} and a peak corresponding to strong N–H stretching of $–NH_2$ at 3559 cm^{-1} were synthesized [TETA][ASP]. Near the wavenumber 3456 cm^{-1}, there was a strong N–H stretching vibration, with a sharp peak at 1621 cm^{-1} and 1395 cm^{-1} corresponding to C=O and carboxylic groups, respectively, as given in Figure 5(b). Similar kinds of peaks can be seen in Figure 5(c-e). Commonly, primary and secondary amines can be seen from the absorption bands in the region 3600 to 3000 cm^{-1} range corresponding to N–H stretching vibration. As reported, N–H plane bending vibrations in NH_3^+ are estimated at 3100, 1300–1550 range, and 1600–1750 cm^{-1} (Khanna & Moorie 1999).

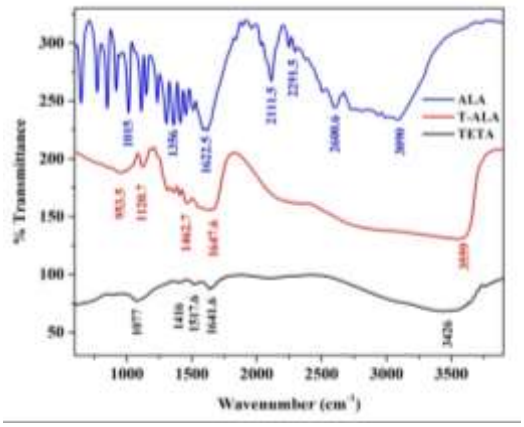

Figure 5(a). FTIR spectra of pure anion $[ALA]^-$, Pure cation $[TETA]^+$, and synthesized [TETA][ALA].

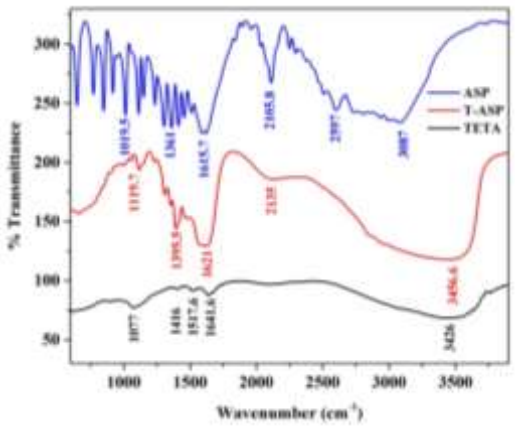

Figure 5(b). FTIR spectra of pure anion $[ASP]^-$, Pure cation $[TETA]^+$, and synthesized [TETA][ASP].

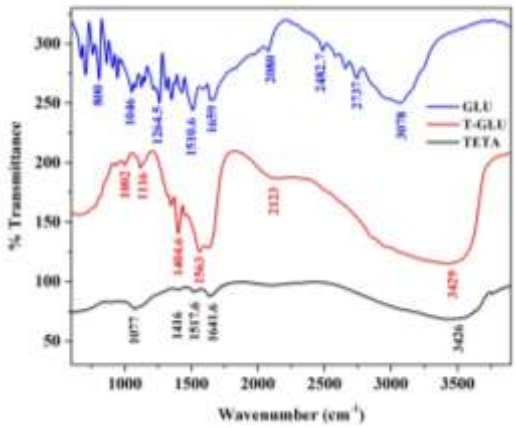

Figure 5(c). FTIR spectra of anion $[GLU]^-$, cation $[TETA]^+$ and synthesized IL [TETA][GLU].

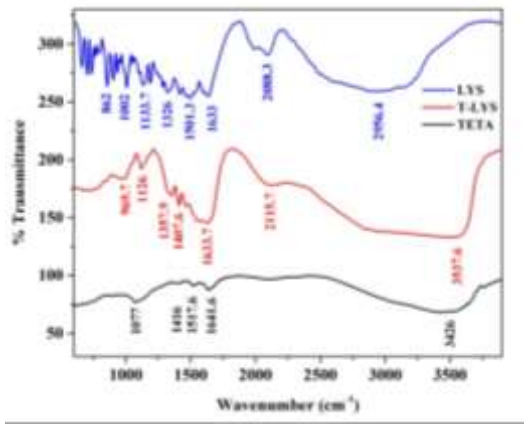

Figure 5(d). FTIR spectra of anion $[LYS]^-$, cation $[TETA]^+$ and synthesized IL [TETA][LYS].

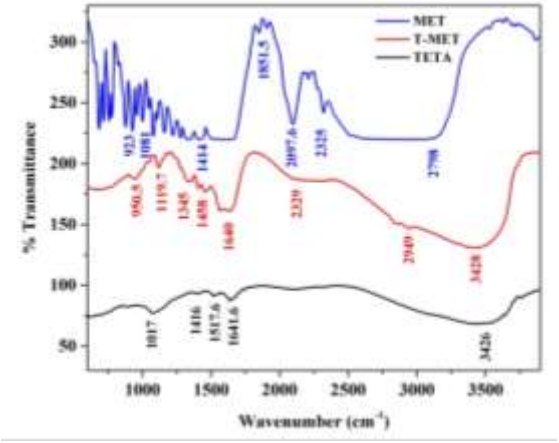

Figure 5(e). FTIR spectra of anion $[MET]^-$, cation $[TETA]^+$ and synthesized IL [TETA][MET].

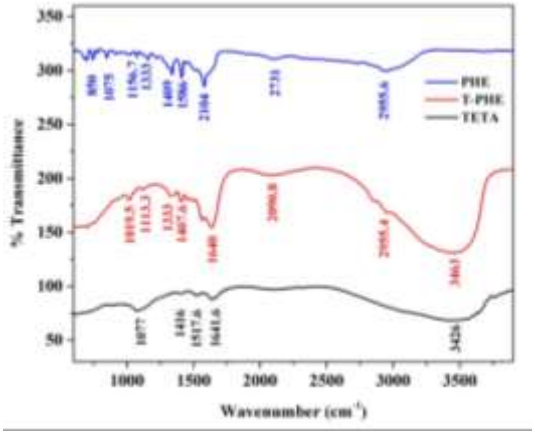

Figure 5(f). FTIR spectra of anion $[PHE]^-$, cation $[TETA]^+$ and synthesized IL [TETA][PHE].

4.1.2. Raman spectroscopy

The synthesized AAILs samples were analyzed using a bench-top Raman spectrometer (Renishaw plc, Model: Micro Raman Spectrometer, RA800-series, UK), equipped with an excitation laser wavelength of 785 nm and about 50% power excitation source. The correctness in the measurement of the wavenumber place of the bands is ±0.98 cm^{-1}, defined by the resolution of the diffraction grating, where the measurement of the intensity usually happens every 1.96 cm^{-1}. Figure 6 represents the Raman spectra of synthesized ILs such as [TETA][LYS], [TETA][GLU], [TETA][ASP], [TETA][ALA], [TETA][MET], [TETA][PHY] and cation $[TETA]^+$.

From Figure 6, the bands found above the 2500 cm^{-1} region are owing to NH, OH, and CH stretching modes for all AAILs. The strongest symmetric stretching of CH_2, $\nu_S(CH_2)$, band in the Raman plot is detected at 2900 to 3100 cm^{-1} (at 2934, 2979, 3030, 3057, and 3073 cm^{-1}) for [TETA][LYS], [TETA][GLU], [TETA][ASP], [TETA][ALA], [TETA][MET] and [TETA][PHE]. It is shifted to the solution state Raman spectrum and is also extremely intense for [TETA][LYS], [TETA][ASP], [TETA][ALA], [TETA][MET] and [TETA][PHE]. Similarly, for pure cation [TETA], it was observed that it was very wide stretching. The stretching of C=C is experiential at 1012, 1033, 1063, and 1076 cm^{-1}; the antisymmetric rocking of NH_3^+ was seen at 1143 and 1183 cm^{-1} for all prepared AAILs. For [TETA][PHE] vibrations associated with the aromatic ring are also detected at 848, 912, and 949 cm^{-1}. A very feature band associated with the C–S stretching was noticed at 659 cm^{-1} since the [TETA][MET] was composed of $C_5H_{11}NO_2S$ and $C_6H_{18}N_4$. Raman spectra of pure amino acids and all synthesized AAILs of individual compounds were given in supporting information (SI Figures 14 to 17).

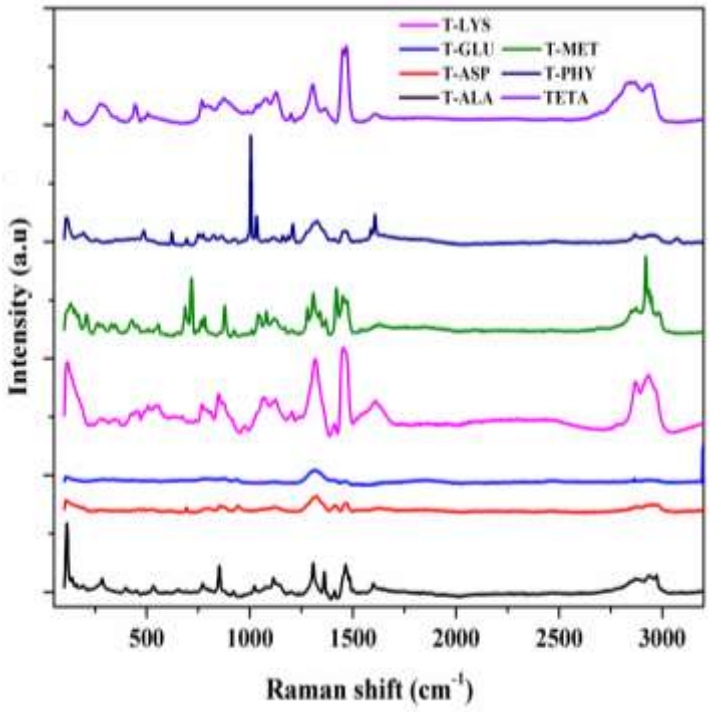

Figure 6. Raman spectra of synthesized ILs [^{TETA}][LYS], [TETA][GLU], [TETA][ASP], [TETA][ALA], [TETA][MET], [TETA][PHE] and cation $[TETA]^+$.

4.1.3. NMR spectroscopy

^{13}C NMR

The ^{1}H and ^{13}C NMR experiments were carried out at ambient temperature using a Bruker Avance 400 or 300 MHz spectrometer. The NMR samples of different synthesized AAILs were prepared with DMSO-d_6 or D_2O. Precautions were taken while preparing the samples to avoid contamination; syringes or capillary tubes were used to transfer the NMR solvent or AAILs.

The peak assignments of ^{13}C NMR data of different synthesized AAILs are as follows (Figure 7(a):

Triethylenetetramine lysine [TETA][LYS]: δc (ppm) (300 MHz, DMSO-D6), 177.96, 54.73, 52.34, 42.23, 36. 58, 30.26, 24.66, 19.44.

Triethylenetetramine glutamine [TETA][GLN]: δc (ppm) (400 MHz, DMSO-D6), 178.0, 56.13, 53.44, 44.90, 36.39, 27.51, 23.14.

Triethylenetetramine aspartic acid [TETA][ASP]: δc (ppm) (300 MHz, DMSO-D6), 174.3, 53.95 50.37, 44.53, 36.29, 34.05.

Triethylenetetramine glutamic acid [TETA][GLU]: δ_c (ppm) (300 MHz, DMSO-D_6), 177.45, 54.22, 50.08, 44.17, 36.08, 29.76, 24.15.

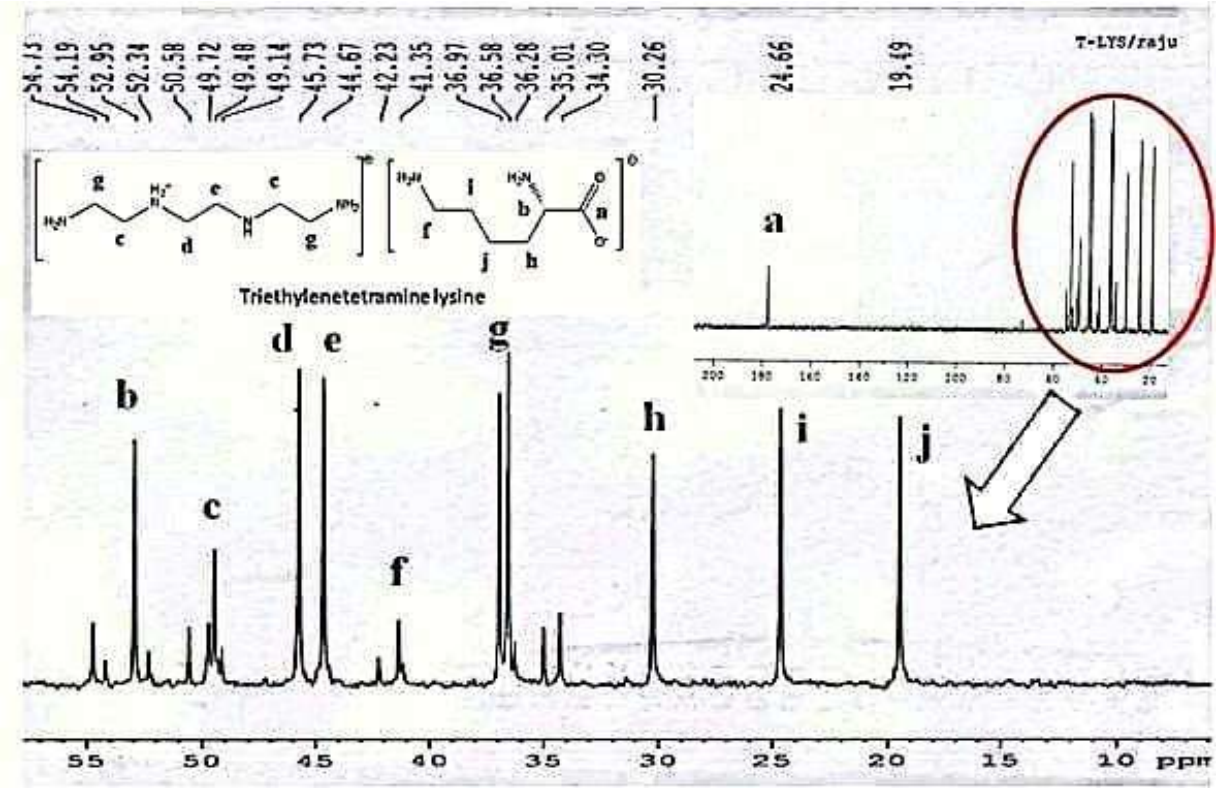

Figure 7(a). Stack plot of ^{13}C NMR spectra of [TETA][LYS] with peak assignment.

^{1}H NMR

The peak assignments of ^{1}H NMR data of different synthesized AAILs are as follows (Figure 7(b):

Triethylenetetramine lysine [TETA][LYS]: δ_H (ppm) (400 MHz, D_2O, the solvent peak was observed at ~ 4.7): 3.4 (s, J = 2.8 Hz, 1H), 2.8, 2.7 (s, J = 2.8 Hz, 1H), 1.59, 1.3 (s, J = 2.8 Hz, 1H).

Triethylenetetramine glutamine [TETA][GLN]: δ_H(ppm) (400 MHz, D_2O, the solvent peak was observed at ~ 4.7): 4.0 (s, J = 2.8 Hz, 2H), 3.5 (s, J = 2.8 Hz, 2H), 2.73 (d, J = 2.8 Hz, 2H).

Triethylenetetramine alanine [TETA][ALA]: δ_H(ppm) (400 MHz, D_2O, solvent peak was observed at ~ 4.76): 3.4 (s, J = 2.8 Hz, 2H), 3.28 (s, J = 2.8 Hz, 2H), 2.60 (s, J = 2.8 Hz, 1H), 2.54 (s, J = 2.8 Hz, 1H).

Triethylenetetramine aspartic acid [TETA][ASP]: δ_H (ppm) (400 MHz, D_2O, the solvent peak was observed at ~ 4.7): 3.6 (s, J = 2.78 Hz, 2H), 2.71 (s, J = 2.8 Hz, 2H), 2.44 (s, J = 2.8 Hz, 1H).

Triethylenetetramine glutamic acid [TETA][GLU]: δ_H (ppm) (400 MHz, D_2O, the solvent peak was observed at ~ 4.7): 3.1 (s, J = 2.8 Hz, 2H), 2.82 (s, J = 2.8 Hz, 2H), 2.65 (s, J = 2.8 Hz, 1H).

The remaining ^{13}C NMR and ^{1}H NMR spectra were given in supporting information (SI Figure 2-13).

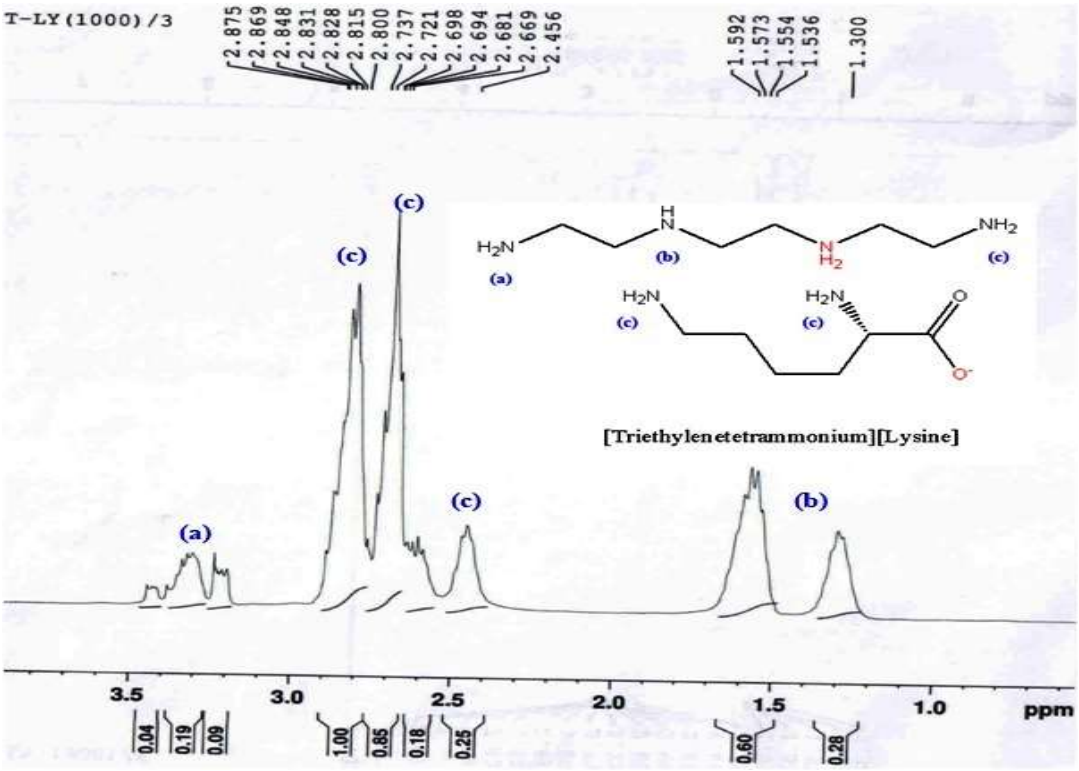

Figure 7(b). Stack plot of ^{1}H NMR spectra of [TETA][LYS] with peak assignment.

The FTIR, Raman, and ^{1}H NMR analyses provide evidence of successful formation of TETA-based AAILs. Characteristic shifts and disappearance of peaks corresponding to free amino acids and unreacted amine groups indicate effective acid–base interaction and conversion. NMR peak assignments have been linked to the expected ionic structures, supporting the proposed formation of the AAILs. While quantitative ^{1}H NMR integration and 2D NMR were not performed, the combined spectroscopic data offer consistent and sufficient confirmation of ionic liquid formation, in line with previous reports on similar systems. These points have now been clarified in the revised manuscript.

4.1.4. Density

Density measurements were performed using a specific gravity bottle of 25 ml volume. A known volume of AAIL was taken in a specific gravity bottle and weighed on an analytical balance at room temperature, and the weights were recorded. The precision of the analytical balance was observed to be ± 0.0001 g. It is known that the density is equal to the mass per unit volume; in a similar way, densities were calculated. Each sample was measured four times; the reproducibility was of a much better order of magnitude. The highest and lowest densities of 1.170 and 1.0646 g cm^{-3} were observed for [TETA][ASP] and [TETA][ALA], among synthesized AAILs respectively. Table 3 depicts the experimentally measured densities of different AAILs at ambient conditions and atmospheric pressure.

Table 3. Experimentally measured densities of AAILs at room temperature and atmospheric pressure.

S. No.	Name of IL	Density (g cm^{-3})	Error
1	[TETA][GLU]	1.1523	0.00153
2	[TETA][ALA]	1.0646	0.00111
3	[TETA][PHE]	1.1468	0.00143
4	[TETA][ASP]	1.1709	0.00066
5	[TETA][LYS]	1.0702	0.00071
6	[TETA][GLN]	-	-
7	[TETA][MET]	-	-

4.1.5. Viscosity measurements

The dynamic viscosity measurements were carried out for all the synthesized ILs as a function of temperature (at 25, 35, 50°C) on a modular compact Rheometer (Anton Paar MCR302 SN81193479) fitted with a Peltier plate at different temperatures using a 40 mm, 2º stainless steel cone. Measurements were done at an angular velocity between an angular velocity of 0.01 and 10 rad s^{-1} and a shear rate of 0 to 200 s^{-1} under ambient conditions. It was found that the viscosity of the IL decreased as the temperature rose. An error of 5% was demonstrated from the manufacturer's data and the analysis on standard liquids; however, reproducibility was better. For ILs studied, the viscosity was moderately constant with increasing the shear rate. This linearity between shear stress and shear rate relates to the Newtonian behavior as described by Huddleston et al., and Seddon et al. (Huddleston et al. 2001, Seddon et al. 2004).

The observed decrease in viscosity with increasing temperature can be attributed to the weakening of hydrogen bonding and other intermolecular interactions within the TETA-based AAILs. ILs such as [TETA][GLU] and [TETA][ALA] exhibit higher viscosities at 25 °C due to more extensive hydrogen bonding networks, which are partially disrupted as the temperature rises, resulting in a sharp drop in viscosity. Compared to benchmark imidazolium- and phosphonium-based ILs and conventional aqueous amine solutions, the TETA-based AAILs maintain moderate viscosities at elevated temperatures, supporting efficient mass transfer and CO_2 absorption in FBR systems (Huddleston et al. 2001, Seddon et al. 2004).

However, missing density values (Table 3) were observed for [TETA][GLN] and [TETA][MET]. These measurements could not be reliably obtained due to the instability and were not stable enough to allow reliable density measurements, and difficulties in handling small sample volumes and the temperature sensitivity of these particular AAILs. Similarly, some viscosity data are missing in Table 4 for [TETA][LYS] (for 25 and 35 °C), [TETA][MET], and [TETA][PHE], as these AAILs did not exhibit stable or consistent behaviour under the measurement conditions. These issues will be addressed in future work.

Table 4. Experimentally measured viscosities of AAILs as a function of temperature and atmospheric pressure.

S. No.	Name of IL	Viscosities (Pa. s)		
		25 (℃)	35 (℃)	50 (℃)
1	[TETA][ASP]	9.8	8.6	4.18
2	[TETA][GLN]	8.53	5.33	3.73
3	[TETA][GLU]	31.6	8.38	1.38
4	[TETA][ALA]	38.3	18.2	7.91
5	[TETA][LYS]	-	-	14.3
6	[TETA][MET]	-	-	-
7	[TETA][PHE]	-	-	-

4.2. CO_2 absorption experiments using a liquid foam bed reactor

The absorption studies were also conducted in a semi-batch liquid foam-bed reactor (FBR) to find the G-L interfacial contact area on the CO_2 absorption rate. The experimental data presented below are at ambient temperature with a bed height of 30 cm. SLS was used in AAILs to generate the foam in FBR. The experiments were carried out in FBR for about 30 min with CO_2 flow rate=2.5×10^{-5} m^3 s^{-1} and airflow rate=8.33×10^{-5} m^3 s^{-1}. Moles of CO_2 absorbed per mole of AAIL use were plotted against the unit time. Several parameters, such as pH, different initial concentrations, the effect of surfactant, regeneration studies, and the use of AAILs after regeneration for multiple cycles, were studied and reported.

The result of the concentration of different AAILs on CO_2 absorption, the desorption performance of different AAILs, and the regenerated AAIL was used for multiple cycles in FBR. Figure 8-11 describes the different initial concentrations of 500, 300, and 100 mmol of AAILs, [TETA][LYS], [TETA][GLU], [TETA][GLN], and [TETA][ASP] were used. It was found that by raising the AAIL concentration, the CO_2 uptake increases up to a certain period because of the increased CO_2 absorption rate.

Figure 8 shows the moles of CO_2 absorbed per mole of [TETA][LYS] used, with the highest mole ratios of 0.442, 0.172, and 0.112, observed in the initial concentration of 500, 300, and 100 mmol, respectively. After 30 min of experimentation, the FBR was saturated, and it reached equilibrium. From Figure 8-11, the highest mole ratio of 0.442 was observed for [TETA][LYS], followed by [TETA][GLN] (0.209) and [TETA][GLU] (0.208) among all used AAILs in this study. The reason for getting the highest mole ratio of CO_2 absorbed per mole of [TETA][LYS] used is that the chemical and physical properties of AAILs differ based on their structural property. Hence, in the case of [TETA][LYS], $[LYS]^-$ anion contains two primary amine groups. Moreover, the higher CO_2 uptake in [TETA][LYS] is primarily attributed to the presence of multiple accessible amine groups and higher basicity, which enhance chemisorption capacity. Additionally, the molecular structure facilitates better accessibility of reactive sites, improving interaction with CO_2 molecules. Similarly, [TETA][GLN] also contains two primary amine groups, which gave the second-highest mole ratio of CO_2 absorbed per mole of

[TETA] [GLN]. A 500 mmol concentration of [TETA][LYS] gave a higher uptake of CO_2 due to the greater number of [TETA][LYS] ions available for reacting with CO_2. Hence, after 30 min [TETA][LYS], available ions were saturated due to the continuous passage of CO_2 and air in the FBR. Because of CO_2 uptake over time, it was noticed that the viscosity of the [TETA][LYS] rises, which in turn decreases the diffusivity of CO_2. During the absorption of CO_2 [TETA][LYS] solution, the initial carbamate was changed to an intermediate form of carbonic acid, i.e. bicarbonate, which may contribute to increased viscosity of the [TETA][LYS]. Similar results were observed for AAILs, [TETA][GLU], [TETA][GLN], and [TETA][ASP] as shown in figure 9-11.

In 2013, Xing et al. reported molecular simulation studies on CO_2 absorption that the difference among amine-based cation ILs and AAILs in terms of ease of use of amines for the ions of ILs. Therefore, there are transformations in the combination of cation and anion interaction and their predictions (Xing et al. 2013). Xing et al. also studied that greater interactions between amine functionalized cations and anions result in decreased interfacial spaces, therefore causing the amine group to a lesser extent of accessibility. In contrast, for AAILs, weaker interactions of the anions with cations make the amine group in the anion more available for CO_2 interaction (Xing et al. 2013). However, the influence of anion–cation interactions on amine accessibility is discussed based on literature reports and has not been directly validated in this study. Therefore, this effect is presented as a reasonable interpretation, and further spectroscopic or computational investigations are required for confirmation.

In this study, the new integrated approach combines the design of TETA-based amino acid ionic liquids (AAILs) with reactor engineering. The presence of multiple active amine sites in TETA enhances CO_2 absorption via chemisorption, while the liquid foam-bed reactor (FBR) provides a high gas–liquid interfacial area, enabling improved mass transfer. This combined strategy aims to maximize CO_2 absorption efficiency by leveraging both material properties and reactor performance.

Amines such as TETA used in ILs as a cation absorb CO_2 via both chemical and physical absorption. The strength of physical absorption mostly relies on the kind of anion used; in this case, it is AAs. Though [LYS] as an anion absorbed CO_2 appreciably by the physisorption, [TETA][LYS] could attain the stoichiometric amount of CO_2 at given experimental conditions due to the limited approachability of amine groups by anion and cation interactions. Figures 8-11 show that for AAILs, chemisorption is the predominant mechanism to a greater extent of predominant mechanism. As reported in the literature, physical absorption in non-functionalized ILs, such as [bmim][BF_4] the less CO_2 molar uptake (Yamini & Khanna, 2015).

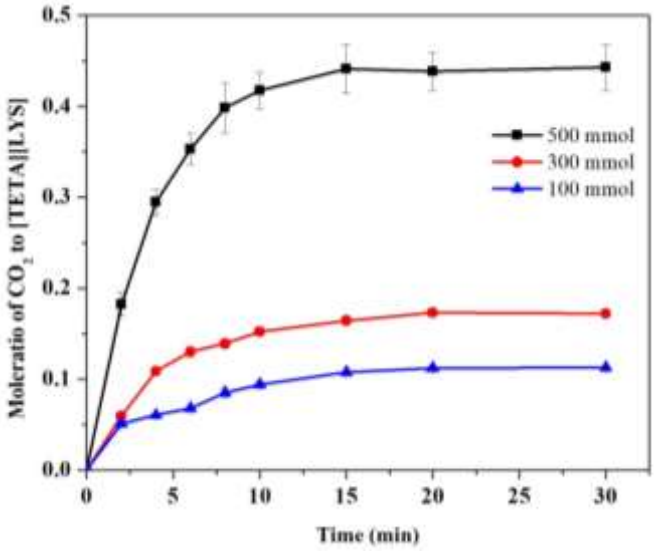

Figure 8. Effect of initial concentration of [TETA][LYS] on CO_2 absorption. [Conditions: Sample volume= 100 ml, SLS added: 0.1 g, initial pH=9.6 (for 100 mmol), 9.46 (for 300 mmol), 9.63 (for 100 mmol), bed height=30 cm, CO_2 flow rate=2.5×10^{-5} m^3 s^{-1} (1.5 LPM), air flow rate=8.33×10^{-5} m^3 s^{-1}(5 LPM), and temperature=~25°C].

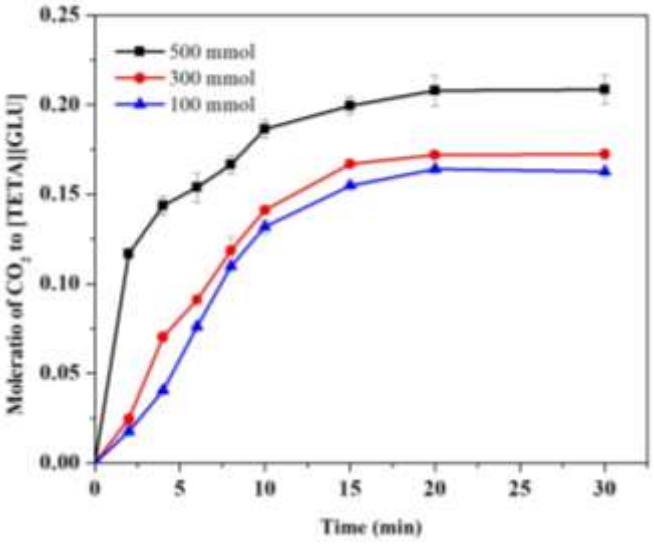

Figure 9. Effect of initial concentration of [TETA][GLU] on CO_2 absorption. [Conditions: Sample volume= 100 ml, SLS added: 0.1 g, initial pH=7.4 (for 100 mmol), 7.46 (for 300 mmol), 7.55 (for 500 mmol), bed height=30 cm, CO_2 flow rate=2.5×10^{-5} m^3 s^{-1} (1.5 LPM), air flow rate=8.33×10^{-5} m^3 s^{-1}(5 LPM), and temperature=~25°C].

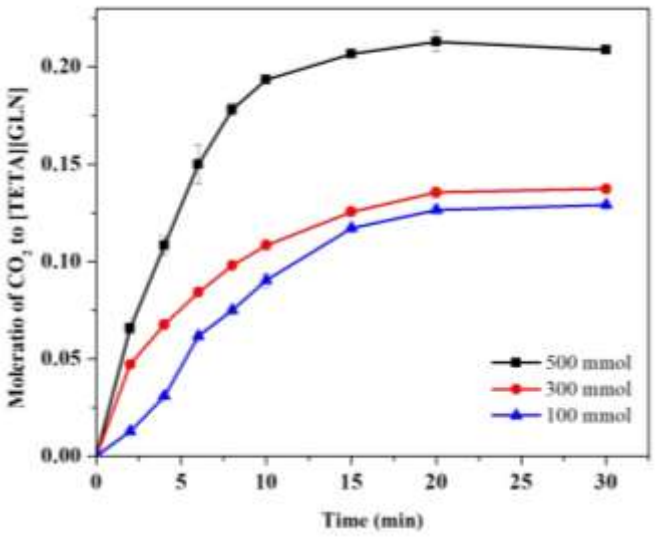

Figure 10. Effect of initial concentration of [TETA][GLN] on CO_2 absorption. [Conditions: Sample volume= 100 ml, SLS added: 0.1 g, initial pH=8.04 (for 100 mmol), 8.3 (for 300 mmol), 9.35 (for 500 mmol), bed height=30 cm, CO_2 flow rate=2.5×10^{-5} m^3 s^{-1} (1.5 LPM), air flow rate=8.33×10^{-5} m^3 s^{-1}(5 LPM), and temperature=~25°C].

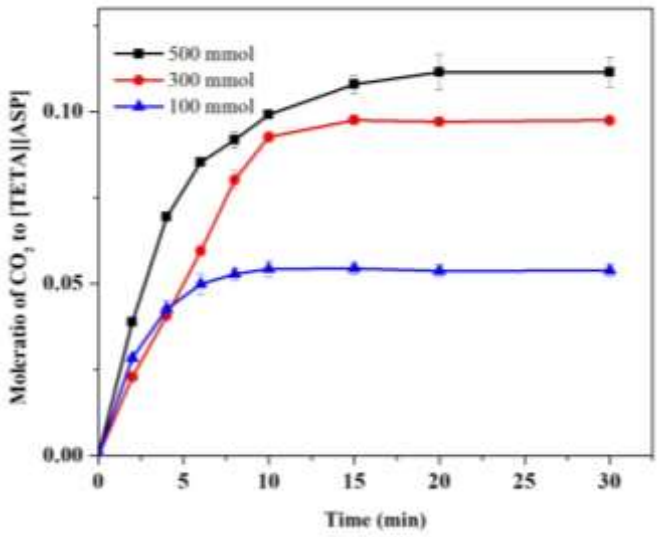

Figure 11. Effect of initial concentration of [TETA][ASP] on CO_2 absorption. [Conditions: Sample volume= 100 ml, SLS added: 0.1 g, initial pH=7.4 (for 100 mmol), 7.46 (for 300 mmol), 7.55 (for 500 mmol), bed height=30 cm, CO_2 flow rate=2.5×10^{-5} m^3 s^{-1} (1.5 LPM) and airflow rate=8.33×10^{-5} m^3 s^{-1} (5 LPM), and temperature=~25°C].

The results of CO_2 absorption in an FBR were compared with results obtained in a bubble-column reactor where no surfactant was used. But in both cases, equal liquid volume was used for the experiment. CO_2 absorption through chemical reactions was described by Bhaskarwar and Kumar. They reported that the FBR gives a higher contact area than a bubble-column reactor (Bhaskarwar & Kumar 1984). According to this study, the average CO_2 absorption rate in FBR was 20% greater than that of the bubble column.

The enhanced CO_2 absorption observed in the FBR compared to the semi-batch equilibrium system (SBES) is attributed to the synergistic effect of material properties and reactor hydrodynamics. The intrinsic characteristics of TETA-based AAILs, including amine functionality, viscosity, and reactivity, significantly influence their performance under different reactor conditions. The FBR system effectively utilizes these properties by increasing interfacial contact, leading to superior absorption performance.

4.3. Effect of surfactant concentration

In this work, different surfactants such as sodium lauryl sulfate (anionic), cetrimonium bromide (cationic), TritonX-100 (nonionic), and Tween 80 (nonionic) were used in FBR for generating the foam. The most stable foam and the highest CO_2 uptake were observed with sodium lauryl sulfate. In the case of Triton X-100 and Tween 80 surfactants, very poor foam generation was observed and unstable when mixing with AAIL during FBR experiments. All the surfactants used were taken based on the CMC values. From the experiments, it was noted that by the addition of more surfactants, the absorption rate was decreased. But below the CMC value (8.2 mM) of SLS, the high concentration of the resistance decreases, and the diffusion flux of CO_2 uptake increases. The CO_2 absorption increases with surfactant concentration up to the CMC, after which further addition may reduce mass transfer efficiency due to excessive foam stabilization. It is acknowledged that quantitative measurements of interfacial area and foam stability were not performed, and this limitation has now been clearly stated remains a subject for future investigation.

Previously, Roy et al. (1997 explained that when the surfactant concentration was enhanced, the solubility of CO_2 in the surfactant solution increased owing to micellar solubilization (Roy et al. 1995. Nonetheless, the amount of dissolved and unreacted CO_2 in the foam film is extremely low in a gas-liquid reacting system. This could lead to the potential for increased CO_2 solubility. However, as the surfactant concentration rose, more surfactant molecules surrounded the gas-film interface, resulting in the creation of several layers. This left a small amount of interfacial surface available for the foam liquid to absorb CO_2. Nevertheless, at high concentrations of surfactants, greater than the CMC value, the micelles opted for cylindrical shapes, which provided some free space for CO_2 absorption, and thus, the absorption rate marginally improved.

4.4. Semi-batch equilibrium experiments

The Semi-batch equilibrium experiments on CO_2 absorption were carried out at room temperature for more than 5 h. [TETA][GLU], [TETA][GLU], and [TETA][ASP] AAIL of 100 mmol concentration with 200 ml volume was chosen for performing the equilibrium experiments. A continuous supply of pure CO_2 bubbling was carried out with stirring. After the equilibrium experiment, AAIL was regenerated and used for further cycles.

Figure 12-14 describes the equilibrium experiments on CO_2 absorption and desorption for [TETA][GLU], [TETA][GLU] and [TETA][ASP. From these studies, it was observed that the reaction involved

in the deprotonation by the water molecule is slow. These experiments revealed that the moles of CO_2 absorbed per mole of AAILs used are less than the FBR experiments due to the smaller interfacial area, and the reaction involved in the de-protonation by the water molecule is slow. From Figure 12-14, moles of CO_2 absorbed per mole of AAIL slightly increase with time, and it reaches equilibrium after about 4-5 h. The ionic liquid was saturated with CO_2 following the completion of an absorption procedure. As explained in the experimental section, desorption investigations were also conducted following the experiment. The weight for the IL was first recorded before the start of the absorption cycle to guarantee the proper desorption of CO_2 from the IL. When all the CO_2 in the CO_2−IL system decomposed, the IL's weight stayed the same. CO_2 was first absorbed into IL until it reached absorption equilibrium, and then it was desorbed from the CO_2-rich IL system. This is known as an absorption-desorption cycle.

During the desorption, the moles of CO_2 absorbed per mole of AAIL decreased with time, and it reached equilibrium after 4 h. From Figure 12, the highest mole ratio of CO_2 per mole of [TETA][GLU] was obtained at 0.166, followed by 0.133 for [TETA][ALA], as shown in Figure 14. Desorption studies were also plotted on the same figures, which are from 0.124 to 0.025-mole ratios of CO_2 per mole of [TETA][GLU], and for [TETA][ALA], it is 0.12 to 0.013, as shown in Figures 12 and 14, respectively. The lowest CO_2 uptake of 0.07 was observed for [TETA][ASP] as represented in Figure 13. Used [TETA][GLU] was carried for another cycle of experiment, which is shown in Figure 15. It can be seen from Figure 15 that [TETA][GLU] used in the first cycle gave the highest mole ratio of CO_2 of 0.166 per mole of AAIL used; in the second cycle, it was 0.121 mole ratio of CO_2 per mole of [TETA][GLU]. This experiment shows that AAILs can be used for multiple cycles after regeneration.

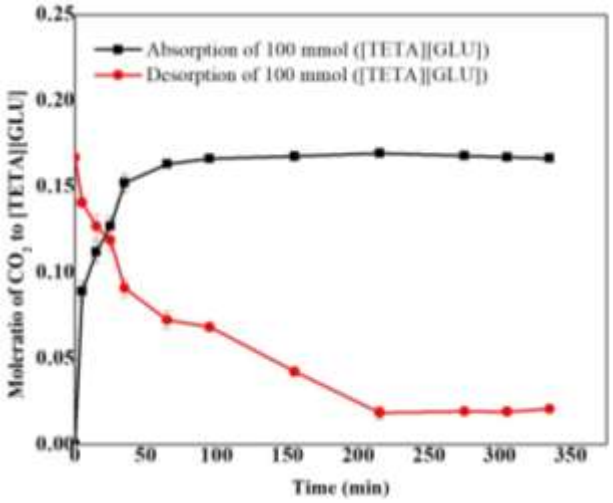

Figure 12. Plot of absorption and desorption of [TETA][GLU] on CO_2 absorption. [Conditions: Sample volume= 200 ml, volume of RBF= 500 ml, initial pH=7.4 (for 100 mmol), CO_2 flow rate=2.5×10^{-5} m^3 s^{-1} (1.5 LPM), stirring speed 80 rpm, temperature=~25°C].

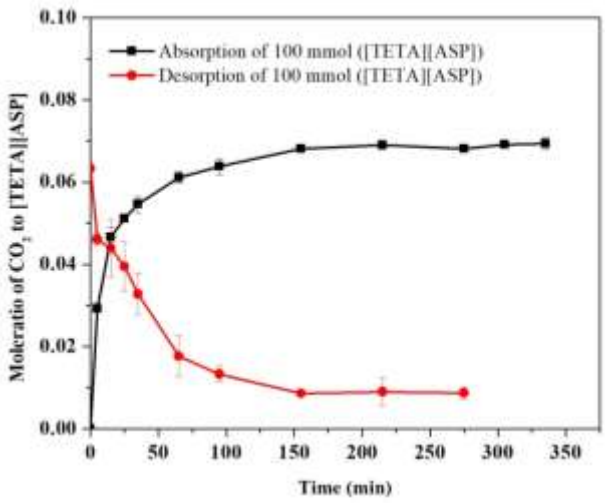

Figure 13. Plot of absorption and desorption of [TETA][ASP] on CO_2 absorption. [Conditions: Sample volume= 200 ml, volume of RBF= 500 ml, initial pH=7.5 (for 100 mmol), CO_2 flow rate=2.5×10^{-5} m^3 s^{-1} (1.5 LPM), stirring speed 80 rpm, temperature=~25°C].

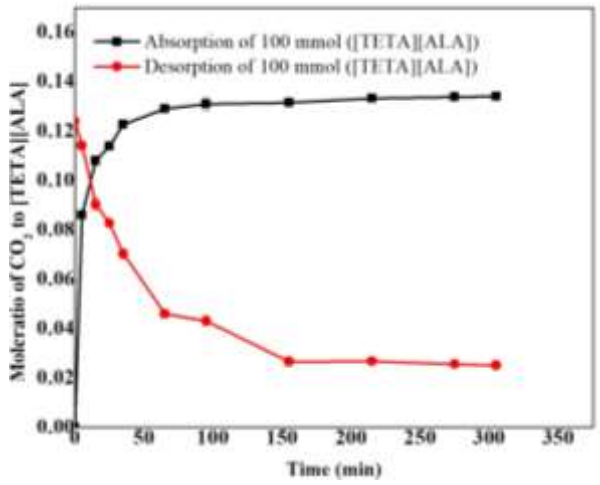

Figure 14. Plot of absorption and desorption of [TETA][ALA] on CO_2 absorption. [Conditions: Sample volume= 200 ml, volume of RBF= 500 ml, initial pH=7.9 (for 100 mmol), CO_2 flow rate=2.5×10^{-5} m^3 s^{-1} (1.5 LPM), stirring speed 80 rpm, temperature=~25℃].

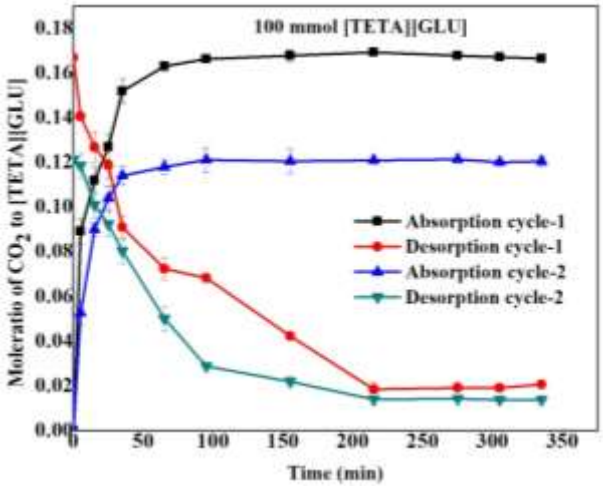

Figure 15. Plot of absorption and desorption of [TETA][GLU] for two different cycles on CO_2 absorption. [Conditions: Sample volume= 200 ml, volume of RBF= 500 ml, initial pH=7.4 (for 100 mmol), CO_2 flow rate=2.5×10^{-5} m^3 s^{-1} (1.5 LPM), stirring speed 80 rpm, temperature=~25℃].

5. CONCLUSIONS

This work describes the synthesis and characterization of CO_2 absorption in an FBR. About seven new ILs namely [TETA][ALA], [TETA][LYS], [TETA][GLU], [TETA][GLN], [TETA][MET], and [TETA][PHE] were synthesized. The characterization of the prepared AAILs was performed using different spectroscopic techniques, such as FTIR, Raman spectroscopy, ^{1}H, and ^{13}C NMR, to confirm the AAILs. Parameters such as the effect of initial concentration, the effect of surfactant, and pH were studied. SLS surfactant was best suited for this study in FBR experiments. Viscosity, density, and surface tension measurements were carried out to present the physical properties of AAILs. The application of AAILs in FBR for the absorption of CO_2 was performed under different experimental conditions. The highest and lowest densities of 1.170 and 1.0646 g cm^{-3} were observed for [TETA][ASP] and [TETA][ALA], respectively, among synthesized AAILs. From the viscosity measurements, it was observed that by increasing the temperature, the viscosity of the AAILs decreased. [TETA][LYS] gave the highest moles of CO_2 absorbed per mole of [TETA][LYS] used; it is reported that the highest mole ratio of 0.442, 0.172, and 0.112 was observed in the initial concentration of 500, 300 and 100 mmol, respectively, AAILs used among all. Regeneration studies were also carried out for multiple uses of AAILs for CO_2 absorption. It was observed that the highest mole ratio of CO_2 per mole of [TETA][GLU] was obtained at 0.166, followed by 0.133 for [TETA][ALA] for desorption studies. FBR and semi-batch equilibrium studies data suggest that amino acids combined with amines are suitable candidates for CO_2 absorption compared with other ionic liquids. The prepared AAILs are bio-degradable, the synthesis procedure was very robust and easy and can be prepared at a low cost compared with conventional commercial ionic liquids.

Author Contributions: Conceptualization, Investigation, Methodology, Writing original draft, data analysis**,** review & editing: Santhi Raju Pilli.

Acknowledgment: The authors gratefully acknowledge the funding of the Deanship of Graduate Studies and Scientific Research, Jazan University, Saudi Arabia Arabia, through Project number: (JU- 202603175 -DGSSR- RP -2026 Research).

The SRP would like to thank Mr. Aman Verma, Mr. Shraban Das, Prakash Choudhary, and Nikhil Chimurkar for their assistance during the experiment. SRP is very thankful to IIT Delhi and Prof. Ashok N. Bhaskarwar for providing research facilities. The authors acknowledge the instrumentation support from CRF and Prof. Sridevi U and her research group of IITD for their timely assistance.

Conflicts of Interest: The authors declare no conflicts of interest.

REFERENCES

Barth, A. (2000) 'The infrared absorption of amino acid side chains,' Progress in Biophysics and Molecular Biology, 74(3–5), pp. 141–173. https://doi.org/10.1016/s0079-6107(00)00021-3.

Babamohammadi, S., Shamiri, A. and Aroua, M.K. (2015) 'A review of CO_2 capture by absorption in ionic liquid-based solvents', *Reviews in Chemical Engineering*, 31, pp. 383–412. DOI:10.1515/revce-2014-0032

Bhaskarwar, A.N. and Kumar, R. (1984) 'Oxidation of sodium sulfide in a foam bed contactor', *Chemical Engineering Science*, 39, pp. 1393–1399. https://doi.org/10.1016/0009-2509(84)80072-X

Cahyonugroho, O.H., Putra, I.S., Hidayah, E.N. and Novembrianto, R. (2025) 'Carbon dioxide gas reduction using the absorp tion method as an effort to support carbon capture and storage (CCS) technology', *Nature Environment and Pollution Technology*, 24(3), p. D1720. https://doi.org/10.46488/NEPT.2025.v24i03.D1720

Cota, I. and Martinez, F.F. (2017) 'Recent advances in the synthesis and applications of metal organic frameworks doped with ionic liquids for CO 2 adsorption,' Coordination Chemistry Reviews, 351, pp. 189–204. https://doi.org/10.1016/j.ccr.2017.04.008.

Danckwerts, P.V. (1979) 'The reaction of CO_2 with ethanolamines', *Chemical Engineering Science*, 34, pp. 443–446. https://doi.org/10.1016/0009-2509(79)85087-3

Du, Y., Yuan, Y. and Rochelle, G.T. (2016) 'Capacity and absorption rate of tertiary and hindered amines blended with piper azine for CO_2 capture', *Chemical Engineering Science*, 155, pp. 397–404. https://doi.org/10.1016/j.ces.2016.08.017

Elmobarak, W.F., Almomani, F., Tawalbeh, M., Al-Othman, A., Martis, R. and Rasool, K. (2023) 'Current status of CO_2 capture with ionic liquids: Development and progress', *Fuel*, 344, 128102. https://doi.org/10.1016/j.fuel.2023.128102.

Fukumoto, K., Yoshizawa, M. and Ohno, H. (2005) 'Room-temperature ionic liquids from 20 natural amino acids', *Journal of the American Chemical Society*, 127, pp. 2398–2399. https://doi.org/10.1021/ja043451i

Goodrich, B.F., de la Fuente, J.C., Gürkan, B.E., Zadigian, D.J., Price, E.A., Huang, Y. and Brennecke, J.F. (2011) 'Experi mental measurements of amine-functionalized anion-tethered ionic liquids with carbon dioxide', *Industrial & Engineering Chemistry Research*, 50, pp. 111–118. https://doi.org/10.1021/ie101688a

Gürkan, B.E., de la Fuente, J.C. and Mindrup, E.M. (2010) 'Equimolar CO_2 absorption by anion-functionalized ionic liquids', *Journal of the American Chemical Society*, 132, pp. 2116–2117. https://doi.org/10.1021/ja909305t

Huddleston, J.G. *et al.* (2001) 'Characterization and comparison of hydrophilic and hydrophobic room temperature ionic liquids incorporating the imidazolium cation,' *Green Chemistry*, 3(4), pp. 156–164. https://doi.org/10.1039/b103275p.

IPCC (2005) *IPCC special report on carbon dioxide capture and storage*. Prepared by Working Group III of the Intergovern mental Panel on Climate Change. Edited by B. Metz, O. Davidson, H.C. de Coninck, M. Loos and L.A. Meyer. Cambridge: Cambridge University Press.

Jones, C.W. (2011) 'CO_2 capture from dilute gases as a component of modern global carbon management', *Annual Review of Chemical and Biomolecular Engineering*, 2, pp. 31–52. https://doi.org/10.1146/annurev-chembioeng-061010-114252

Khanna, R.K. and Moorie, M.H. (1999) 'Carbamic acid: Molecular structure and IR spectra', *Spectrochimica Acta Part A*, 55, pp. 961–967. https://doi.org/10.1016/S1386-1425(98)00228-5

Kortunov, P.V., Baugh, L.S. and Siskin, M. (2015) 'Pathways of the chemical reaction of carbon dioxide with ionic liquids and amines in ionic liquid solution', *Energy & Fuels*, 29, pp. 5990–6007. https://doi.org/10.1021/acs.energyfuels.5b00876

Kumar, P.S., Hogendoorn, J.A., Feron, P.H.M. and Versteeg, G.F. (2002) 'New absorption liquids for the removal of CO_2 from dilute gas streams using membrane contactors', *Chemical Engineering Science*, 57, pp. 1639–1651. https://doi.org/10.1016/S0009-2509(02)00041-6

Kumar, P.S., Hogendoorn, J.A. and Versteeg, G.F. (2003) 'Kinetics of the reaction of CO_2 with aqueous potassium salts of taurine and glycine', *AIChE Journal*, 49, pp. 203–213. https://doi.org/10.1002/aic.690490118

Lupa, L., Tolea, N.S., Iosivoni, M., Măranescu, B., Pleșu, N. and Visa, A. (2024) 'Performance of ionic liquid functionalized metal–organic frameworks in the adsorption process of phenol derivatives', *RSC Advances*, 14, pp. 4759–4777. https://doi.org/10.1039/d3ra08024b.

Makino, T. and Kanakubo, M. (2016) 'CO_2 absorption property of ionic liquid and CO_2 permselectivity for ionic liquid mem brane', *Journal of the Japan Petroleum Institute*, 59, pp. 109–117. https://doi.org/10.1627/jpi.59.109

Mandal, B.P. and Bandyopadhyay, S.S. (2005) 'Simultaneous absorption of carbon dioxide and hydrogen sulfide into aqueous blends of 2-amino-2-methyl-1-propanol and diethanolamine', *Chemical Engineering Science*, 60, pp. 6438–6451. https://doi.org/10.1016/j.ces.2005.02.044

Mohamedali, M., Ibrahim, H. and Henni, A. (2017) 'Incorporation of acetate-based ionic liquids into a zeolitic imidazolate framework (ZIF-8) as efficient sorbents for carbon dioxide capture,' Chemical Engineering Journal, 334, pp. 817–828. https://doi.org/10.1016/j.cej.2017.10.104.

Mulk, W.U., Ali, S.A., Shah, S.N., Shah, M.U.H., Zhang, Q.J., Younas, M., Fatehizadeh, A., Sheikh, M. and Rezakazemi, M. (2023) 'Breaking boundaries in CO_2 capture: Ionic liquid-based membrane separation for post-combustion applications', *Journal of CO_2 Utilization*, 75, 102555. https://doi.org/10.1016/j.jcou.2023.102555

Mumford, K.A., Mirza, N.R. and Stevens, G.W. (2017) 'Review: Room-temperature ionic liquids and system designs for CO_2 capture', *Energy Procedia*, 114, pp. 2671–2674. https://doi.org/10.1021/acs.energyfuels.4c02513

Norouzbahari, S., Shah Hosseini, S. and Ghaemi, A. (2016) 'Chemical absorption of CO_2 into aqueous piperazine (PZ) solu tion: Development and validation of a rigorous dynamic rate-based model', *RSC Advances*, 6, pp. 40017–40032. https://doi.org/10.1039/C5RA27869D

Padmanabhan, S., Joel, C., Mahalingam, S., Deepak, J.R., Kumar, T.V. and Raj, D. (2024) 'An overview of the need for circular economy on electric vehicle batteries', *Nature Environment and Pollution Technology*, 23(1), pp. 183–191. https://doi.org/10.46488/NEPT.2024.v23i01.014

Pilli, S.R., Banerjee, T. and Mohanty, K. (2014) 'Liquid–liquid equilibrium (LLE) data for ternary mixtures of [C_4DMIM][PF_6]–[PCP]–water and [C_4DMIM][PF_6]–[PA]–water at T = 298.15 K and p = 1 atm', *Fluid Phase Equilibria*, 381, pp. 12–19. doi: 10.1016/j.fluid.2014.08.004

Qu, Y., Chen, Y., Ye, Y., Xu, P. and Sun, J. (2022) 'Supercritical CO_2-assisted synthesis of SBA-15-supported amino acid ionic liquid for CO_2 cycloaddition under cocatalyst-, metal- and solvent-free conditions', *Journal of CO_2 Utilization*, 66, 102294. https://doi.org/10.1016/j.jcou.2022.102294.

Ramdin, M., de Loos, T.W. and Vlugt, T.J.H. (2012) 'State-of-the-art of CO_2 capture with ionic liquids', *Industrial & Engi neering* Chemistry *Research*, 51, pp. 8149–8177. https://doi.org/10.1021/ie3003705

Roy, D., Kommalapati, R.R., Valsaraj, K.T. and Constant, W.D. (1995) 'Soil flushing of residual transmission fluid: Application of colloidal gas aphron suspensions and conventional surfactant solutions', *Water Research*, 29, pp. 589–595. doi:10.1016/0043-1354(94)00171-3

Sarker, A.I., Aroonwilas, A. and Veawab, A. (2017) 'Equilibrium and kinetic behaviour of CO_2 adsorption onto zeolites, carbon molecular sieve and activated carbons', *Energy Procedia*, 114, pp. 2450–2459. https://doi.org/10.1016/j.egypro.2017.03.1394

Seddon, R., Stark, A.S. and Torres, M.J. (2004) 'Viscosity and density of 1-alkyl-3-ethylimidazolium ionic liquids', in Rogers, R.D. and Seddon, K.R. (eds.) *Ionic liquids III: Fundamentals, progress, challenges, and opportunities*. ACS Symposium Series 901. Washington, DC: American Chemical Society. doi:10.1021/bk-2002-0819.ch004

Sun, J., Li, X., Yu, K. and Yin, J. (2022) 'A novel supported ionic liquid membrane reactor for catalytic CO_2 conversion', *Journal of* CO_2 *Utilization*, 65, 102216. https://doi.org/10.1016/j.jcou.2022.102216.

van Holst, G.F.V., Brilman, D.W.F. and Hogendoorn, J.A. (2009) 'Kinetic study of CO_2 with various amino acid salts in aqueous solution', *Chemical Engineering Science*, 64, pp. 59–68. https://doi.org/10.1016/j.ces.2008.09.015

Versteeg, G.F. and van Swaaij, W.P.M. (1988) 'On the kinetics between CO_2 and alkanolamines both in aqueous and non-aqueous solutions—I. Primary and secondary amines', *Chemical Engineering Science*, 43, pp. 573–585. https://doi.org/10.1016/0009-2509(88)87018-0

Wahby, J., Silvestre-Albero, A., Sepúlveda-Escribano, A. and Rodríguez-Reinoso, F. (2012) 'CO_2 adsorption on carbon molecular sieves', *Microporous and Mesoporous Materials*, 164, pp. 280–287. https://doi.org/10.1016/j.micromeso.2012.06.034

Walden, P. (1914) 'Molecular weights and electrical conductivity of several fused salts', *Bulletin of the Imperial Academy of Sciences (Saint Petersburg)*, 1800, pp. 405–422. https://ci.nii.ac.jp/naid/10025720020/

Wilkes, J.S. (2002) 'A short history of ionic liquids: From molten salts to neoteric solvents', *Green Chemistry*, 4, pp. 73–80. https://doi.org/10.1039/B110838G

Xie, H.B., Zhou, Y., Zhang, Y. and Johnson, J.K. (2010) 'Reaction mechanism of monoethanolamine with CO_2 in aqueous solution from molecular modelling', *Journal of Physical Chemistry A*, 114, pp. 11844–11852. https://doi.org/10.1021/jp107516k

Xing, H., Yan, Y., Yang, Q., Bao, Z., Su, B., Yang, Y. and Ren, Q. (2013) 'Effect of tethering strategies on the surface structure of amine-functionalized ionic liquids: Inspiration on the CO_2 capture', *Journal of Physical Chemistry C*, 117, pp. 16012–16021. https://doi.org/10.1021/jp402497s

Yamini, S.S. and Khanna, A. (2014) 'Carbon dioxide absorption studies using amine-functionalized ionic liquids', *Journal of Industrial and Engineering Chemistry*, 20, pp. 2497–2509. https://doi.org/10.1016/j.jiec.2013.10.032

Yamini, S.S. and Khanna, A. (2015) 'CO_2 absorption studies in amino acid-anion-based ionic liquids', *Chemical Engineering Journal*, 273, pp. 268–276. https://doi.org/10.1016/j.cej.2014.09.043

Zhang, L.-L., Wang, J.-X., Xiang, Y., Zeng, X.-F. and Chen, J.-F. (2011) 'Absorption of carbon dioxide with ionic liquid in a rotating packed bed contactor: Mass transfer study', *Industrial & Engineering Chemistry Research*, 50, pp. 6957–6964. https://doi.org/10.1021/IE1025979